Cyclin G and the Polycomb Repressive Complexes PRC1 and PR-DUB cooperate for developmental stability.

Delphine Dardalhon-Cuménal[1,2], Jérôme Deraze[1,2], Camille A Dupont[1,2], Valérie Ribeiro[1,2], Anne Coléno-Costes[1,2], Juliette Pouch[4], Stéphane Le Crom [4,5], Hélène Thomassin[1,2], Vincent Debat[3], Neel B Randsholt[1,2] and Frédérique Peronnet[1,2].

[1] Sorbonne Universités, UPMC Univ Paris 06, Institut de Biologie Paris-Seine (IBPS), UMR 7622, Developmental Biology, F-75005, Paris, France

[2] CNRS, IBPS, UMR 7622, Developmental Biology, F-75005, Paris, France

[3] Museum national d'Histoire naturelle, Institut de Systématique, Évolution, Biodiversité, ISYEB UMR 7205, CNRS-MNHN-UPMC-EPHE, Sorbonne Universités, 45 rue Buffon, 75005 Paris, France

[4] IBENS, Département de Biologie, Ecole Normale Supérieure, CNRS, Inserm, PSL Research University, F‑75005 Paris, France

[5] Sorbonne Universités, UPMC Univ Paris 06, Univ Antilles, Univ Nice Sophia Antipolis, CNRS, Evolution Paris Seine - Institut de Biologie Paris Seine (EPS - IBPS), 75005 Paris, France

Keywords : *Drosophila melanogaster*, Developmental Stability, Fluctuating Asymmetry, Developmental noise, Polycomb, Cyclin G

ABSTRACT

In *Drosophila*, ubiquitous expression of a short Cyclin G isoform generates extreme developmental noise estimated by fluctuating asymmetry (FA), providing a model to tackle developmental stability. This transcriptional cyclin interacts with chromatin regulators of the Enhancer of Trithorax and Polycomb (ETP) and Polycomb families. This led us to investigate the importance of these interactions in developmental stability. Deregulation of Cyclin G highlights an organ intrinsic control of developmental noise, linked to the ETP-interacting domain, and enhanced by mutations in genes encoding members of the Polycomb Repressive complexes PRC1 and PR-DUB. Deep-sequencing of wing imaginal discs deregulating *CycG* reveals that high developmental noise correlates with up-regulation of genes involved in translation and down-regulation of genes involved in energy production. Most Cyclin G direct transcriptional targets are also direct targets of PRC1 and RNAPolII in the developing wing. Altogether, our results suggest that Cyclin G, PRC1 and PR-DUB cooperate for developmental stability.

INTRODUCTION

Developmental stability has been described as the set of processes that buffer disruption of developmental trajectories for a given genotype within a particular environment (Palmer, 1994). In other words, developmental stability compensates the random stochastic variation of processes at play during development. Many mechanisms working from the molecular to the whole organism levels contribute to developmental stability (Nijhout and Davidowitz, 2003). For example, chaperones, such as heat-shock proteins, participate in developmental stability in a large variety of developmental processes by protecting misfolded proteins from denaturation (Feder and Hofmann, 1999; Queitsch et al., 2002; Rutherford et al., 2007). In *Drosophila melanogaster*, adjustment of cell growth to cell proliferation is essential to developmental stability by allowing to achieve a consistant organ size (*e.g.* wing size) in spite of variation in cell size or cell number (Debat et al., 2011; Debat and Peronnet, 2013).

Developmental noise, the “sum” of the stochastic part of each developmental process, can be observed macroscopically for morphological traits. In bilaterians, quantification of departure from perfect symmetry, the so-called fluctuating asymmetry (FA), is the most commonly used index to estimate developmental noise (Van Valen, 1962; Palmer and Strobeck, 1992). Indeed, the two sides of bilaterally symmetrical traits are influenced by the same genotype and environmental conditions, and differences between them are thus only due to developmental noise. The use of FA as an index of developmental noise makes analysis of the mechanistic and genetic bases of developmental stability compatible with custom genetic and molecular approaches of developmental biology.

The evolutionary role of developmental stability is subject to many speculations (*e.g.* Dongen, 2006) as its genetic bases remain unclear (for reviews see Leamy and Klingenberg, 2005; Debat and Peronnet, 2013). Experiments showing the role of *Hsp90* in buffering genetic variation led to the idea that developmental stability could be ensured by specific genes (Rutherford and Lindquist, 1998; Milton et al., 2003; Debat et al., 2006; Yeyati et al., 2007; Sangster et al., 2008). On the other hand, both theory and experiments show that complex genetic networks can become intrinsically robust to perturbations, notably through negative and positive feedbacks, suggesting that the topology of gene networks is of

paramount importance for developmental stability (Barabasi and Albert, 1999; Siegal and Bergman, 2002; Newman, 2003; Kitano, 2004). Several authors have further suggested that hubs, *i.e.* the most connected genes in these networks, might be particularly important for developmental stability (Rutherford et al., 2007; Levy and Siegal, 2008).

In *Drosophila*, mutants for *dILP8* and *hid*, two genes involved in the control of systemic growth and apoptosis respectively, have been reported to display high FA as compared to wild type flies from the same genetic background (Garelli et al., 2012; Colombani et al., 2012; Neto-Silva et al., 2009), suggesting that these genes are important for developmental stability. Two studies have scanned the *Drosophila* genome for regions involved in developmental stability using FA as an estimator of developmental noise (Breuker et al., 2006; Takahashi et al., 2011). Several deletions increased FA but the genes responsible for this effect inside the deletions were not identified. Nevertheless, these studies confirm that the determinism of developmental stability could well be polygenic, as suggested by Quantitative Trait Loci analyses in mouse (Leamy et al., 2002; Leamy et al., 2005; Leamy et al., 2015). Together, these data reinforce the idea that developmental stability depends on gene networks.

We have shown that the gene *Cyclin G* (*CycG*) of *Drosophila melanogaster*, which encodes a protein involved in transcriptional regulation and in the cell cycle, is important for developmental stability (Salvaing et al., 2008a; Faradji et al., 2011; Debat et al., 2011; Dupont et al., 2015). Indeed, ubiquitous expression of a short Cyclin G version lacking the C-terminal PEST-rich domain ($CycG^{\Delta P}$) generates a very high FA in several organs, notably in the wing. Interestingly, FA induced by $CycG^{\Delta P}$ expression correlates with high variability in cell size and loss of correlation between cell size and cell number, suggesting that the noisy process would somehow be connected to cell cycle related cell growth (Debat et al., 2011). Hence, *CycG* deregulation provides a convenient sensitized system to tackle the impact of cell growth variability on developmental stability.

We previously showed that *CycG* encodes a transcriptional cyclin and interacts with genes of the *Polycomb-group* (*PcG*), *trithorax-group* (*trxG*), and *Enhancer of Trithorax and Polycomb* (*ETP*) families (Salvaing et al., 2008a; Salvaing et al., 2008b; Dupont et al., 2015) . These genes encode evolutionary conserved proteins assembled into large multimeric complexes that bind chromatin. They ensure maintenance of gene expression patterns during development (for recent

reviews see Grossniklaus and Paro, 2014; Kingston and Tamkun, 2014; Geisler and Paro, 2015). *PcG* genes are involved in long-term gene repression, whereas *trxG* genes maintain gene activation and counteract *PcG* action. *ETP* genes encode co-factors of both *trxG* and *PcG* genes, and behave alternatively as repressors or activators of target genes (Gildea et al., 2000; Grimaud et al., 2006; Beck et al., 2010). More recently, we discovered that *CycG* behaves as an *Enhancer of Polycomb* regarding homeotic gene regulation suggesting that it is involved in the silencing of these genes (Dupont et al., 2015). Importantly, Cyclin G physically interacts with the ETP proteins Additional Sex Comb (ASX) and Corto *via* its N-terminal ETP-interacting domain, and co-localizes with them on polytene chromosomes at many sites (Salvaing et al., 2008a; Dupont et al., 2015) . Hence, Cyclin G and these ETPs might share many transcriptional targets and might in particular control cell growth *via* epigenetic regulation of genes involved in growth pathways.

Here, we investigate in depth the role of *CycG* in developmental stability. We first show that localized expression of $CycG^{\Delta P}$ in wing imaginal discs is necessary and sufficient to induce high FA of adult wings. Furthermore, this organ-autonomous effect increases when the ETP-interacting domain of Cyclin G is removed. We show that several mutations for *PcG* or *ETP* genes, notably those encoding members of the PRC1 and PR-DUB complexes, substantially increase *CycG*-induced FA. Next, we report analysis of the transcriptome of wing imaginal discs expressing $CycG^{\Delta P}$ by RNA-seq and find that transcriptional deregulation of genes involved in translation and energy production correlates with high FA of adult wings. By ChIP-seq, we identify Cyclin G binding sites on the whole genome in wing imaginal discs. Strikingly, we observe a significant overlap with genes also bound by ASX, by the Polycomb Repressive complex PRC1, and by RNAPolII in the same tissue. We identify a sub-network of 222 genes centred on Cyclin G showing simultaneous up-regulation of genes involved in translation and down-regulation of genes involved in mitochondrial activity and metabolism. Taken together, our data suggest that Cyclin G and the Polycomb complexes PRC1 and PR-DUB cooperate in sustaining developmental stability. Precise regulation of genes involved in translation and energy production might be important for developmental stability.

RESULTS

Expression of *CycG$^{\Delta P}$* in wing precursors is necessary and sufficient to induce high wing FA

We previously reported that expression of *CycG* deleted of the PEST-rich C-terminal domain (amino-acids 541 to 566) (*CycG$^{\Delta P}$*) under control of ubiquitous drivers (*da-Gal4* or *Actin-Gal4*) generated extremely high FA, notably in wings (Debat et al., 2011) (Figure 1). The strength of this effect was unprecedented in any system or trait. Expression of *CycG$^{\Delta P}$* thus provides a unique tool to investigate developmental stability in depth. To determine whether wing FA was due to local or systemic expression of *CycG$^{\Delta P}$*, we tested a panel of Gal4 drivers specific for wing imaginal discs or neurons. A brain circuit which relays information for bilateral growth synchronization was recently identified (Vallejo et al., 2015). It notably involves a pair of neurons expressing the dILP8 receptor that connects with the insulin-producing cells (IPCs) and the prothoracicotropic hormone (PTTH) neurons. This circuit was particularly appropriate to test the existence of a remote effect of *CycG$^{\Delta P}$* expression in generating high FA in the wing. Expression of *CycG$^{\Delta P}$* in this circuit (using *dilp3-*, *NPF-*, *pdf-, per-, phm-* and *R19B09-Gal4* drivers) did not increase FA of adult wings (Figure 2 and Table 1). Furthermore, expression of *CycG$^{\Delta P}$* in cells of the future wing hinge using the *ts-Gal4* driver did not affect wing FA either. By contrast, expressing *CycG$^{\Delta P}$* with 5 different wing pouch drivers (*nub-, omb-, rn-, sd-* and *vg-Gal4*) induced high FA. We thus concluded that *CycG$^{\Delta P}$*-induced wing FA was due to an intrinsic response of the growing wing tissue.

The Cyclin G ETP interacting domain sustains developmental stability

The 566 amino-acid Cyclin G protein exhibits 3 remarkable domains: the ETP-interacting domain (amino-acids 1 to 130) that physically interacts with the ETPs Corto and ASX, a cyclin domain (amino-acids 287 to 360) that presents high similarity with the cyclin domain of vertebrate G-type cyclins, and a PEST-rich domain (amino-acids 541 to 566) (Salvaing et al., 2008a; Faradji et al., 2011; Dupont et al., 2015). To test whether the interaction with ETPs (and thus transcriptional regulation by Cyclin G) could be important to control FA, we generated new transgenic lines enabling to express different versions of the *CycG* cDNA: *CycG^{FL}* (encoding the full-length protein), *CycG$^{\Delta E}$* (encoding an ETP-interacting domain deleted protein), *CycG$^{\Delta P}$* (encoding a PEST domain deleted protein), and *CycG$^{\Delta E\Delta P}$*

(encoding an ETP-interacting and PEST domain deleted protein). In order to express these different cDNAs at the same level and compare the amounts of FA induced, all transgenes were integrated at the same site using the *PhiC31* integrase system (at position 51C on the second chromosome). Expression of these transgenic lines was ubiquitously driven by *da-Gal4*. We first confirmed that expression of $CycG^{\Delta P}$ induced very high FA as compared to *yw* and *da-Gal4/+* controls. Furthermore, expression of $CycG^{FL}$ also significantly increased FA, although to a much lesser extent. Interestingly, expression of either $CycG^{\Delta E}$ or $CycG^{\Delta E \Delta P}$ significantly increased FA as compared to $CycG^{FL}$ or $CycG^{\Delta P}$, respectively (Figure 3 and Table 2). These results show that the ETP interacting domain tends to limit Cyclin G-induced FA and suggest that the interaction between Cyclin G and chromatin regulators sustains developmental stability.

CycG and *PcG* or *ETP* genes interact for developmental stability

We next addressed genetic interactions between *CycG* and *PcG* or *ETP* genes for developmental stability. The alleles used are listed in Table 3. FA of flies heterozygous for *PcG* and *ETP* loss of function alleles was not significantly different from that of control flies. However, when combined with a *da-Gal4, UAS-*$CycG^{\Delta P}$ chromosome, many of these mutations significantly increased wing FA as compared to *da-Gal4, UAS-*$CycG^{\Delta P}$ flies (Figure 4 and Table S1). This was notably the case for alleles for PRC1 and PR-DUB encoding genes, the *PcG* genes *Sex comb extra* (Sce^{1}, Sce^{33M2} and Sce^{KO4}), *calypso* ($caly^{1}$ and $caly^{2}$), *Sex comb on midleg* (Scm^{D1}), *Polycomb* (Pc^{1}), and *polyhomeotic* ($ph\text{-}p^{410}$ and $ph\text{-}d^{401}ph\text{-}p^{602}$). No modification of $CycG^{\Delta P}$-induced FA was observed with the Psc^{1} allele. However, this allele has been described as a complex mutation with both loss and gain of function features (Adler et al., 1989).

Opposite effects were observed for different alleles of ETPs *Asx* and *corto.* Asx^{22P4} increased *da-Gal4, UAS-*$CycG^{\Delta P}$ FA whereas Asx^{XF23} decreased it. Asx^{XF23} behaves genetically as a null allele but has not been molecularly characterized (Simon et al., 1992), whereas the Asx^{22P4} allele does not produce any protein and thus likely reflects the effect of loss of ASX (Scheuermann et al., 2010). Similarly, the $corto^{L1}$ allele increased $CycG^{\Delta P}$-induced FA whereas the $corto^{420}$ allele had no effect. In order to characterize these *corto* alleles, we combined them with the *Df(3R)6-7* deficiency that uncovers the *corto* locus, amplified the region by PCR and sequenced

it. The *corto*^{420} allele corresponds to a substitution of 14,209 nucleotides starting at position -59 upstream of the *corto* Transcriptional Start Site (TSS) by a 30-nucleotide sequence. Hence, this allele does not produce any truncated protein. By contrast, *corto*^{L1} corresponds to a C towards T substitution that introduces a stop codon at position +73 downstream the TSS, generating a 24 amino-acid polypeptide. *corto*^{L1} might then behave as a dominant-negative mutation. Lastly, no modification of *CycG*$^{\Delta P}$-induced FA was observed for *E(z)*^{63} and *esc*^{21}.

Interestingly, *Asx* and *caly* encode proteins of the Polycomb Repressive complex PR-DUB whereas *Pc*, *ph*, *Sce* and *Scm* encode proteins of the Polycomb Repressive complex PRC1, and *E(z)* and *esc* encode proteins of the Polycomb Repressive complex PRC2. Taken together, these results indicate that Cyclin G interacts with the Polycomb complexes PRC1 and PR-DUB, but not with PRC2, for developmental stability.

Expression of *CycG*$^{\Delta P}$ or *CycG*$^{\Delta E \Delta P}$ does not modify the bulk of H2AK118ub

Cyclin G binds polytene chromosomes at many sites and co-localizes extensively with PH and ASX suggesting a potential interaction with the PRC1 and PR-DUB complexes on chromatin (Salvaing et al., 2008a; Dupont et al., 2015). The two genes *Sce* and *caly* encode antagonistic enzymes of the PRC1 and PR-DUB complexes, respectively. SCE, aka dRing, ubiquitinates histone H2A on lysine 118 (H2AK118ub) whereas Calypso, aka dBap1, is the major deubiquitinase of the same H2A residue (Scheuermann et al., 2010; Scheuermann et al., 2012). To investigate whether Cyclin G was related to these ubiquitin ligase/deubiquitinase activities, we immunostained polytene chromosomes from *w*^{1118} larvae with anti-Cyclin G and anti-human H2AK119ub antibodies (homologous to *Drosophila* H2AK118ub) (Pengelly et al., 2015). Cyclin G and H2AK118ub co-localized extensively on chromosome arms suggesting that Cyclin G transcriptional activity might somehow be connected to the presence of this histone mark (Figure S1A). However, when either *CycG*$^{\Delta P}$ or *CycG*$^{\Delta E \Delta P}$ was expressed in the posterior compartment of wing imaginal discs using the *en-Gal4* driver, the global amount of H2AK118ub was not markedly modified (Figure S1B, Figure S1C). We thus concluded that high FA was not related to a global perturbation of H2AK118 ubiquitination level.

Cyclin G controls the expression of genes involved in translation and energy production

Cyclin G controls the transcription of the homeotic gene *Abdominal-B* and more specifically behaves as an *Enhancer of PcG* gene in the regulation of homeotic gene expression (Salvaing et al., 2008b; Dupont et al., 2015). However, the high number of Cyclin G binding sites on polytene chromosomes suggests that this cyclin has many other transcriptional targets. We thus hypothesized that the high FA induced by expression of $CycG^{\Delta P}$ might be related to the deregulation of Cyclin G transcriptional targets. To further address the role of Cyclin G in transcriptional regulation, we deep-sequenced the transcripts from wing imaginal discs of *da-Gal4, UAS-*$CycG^{\Delta P}$*/+* and *da-Gal4/+* third instar larvae. Sequence reads were aligned with the *Drosophila melanogaster* genome to generate global gene expression profiles. We performed differential analyses to obtain expression changes for *da-Gal4, UAS-*$CycG^{\Delta P}$*/+* as compared to the *da-Gal4/+* control. With an adjusted p-value threshold of 0.05, we retrieved 530 genes whose expression was significantly different between the two genotypes (Table S2). Surprisingly, expression of *CycG* was only weakly induced in *da-Gal4, UAS-*$CycG^{\Delta P}$*/+* imaginal discs as compared to *da-Gal4/+* imaginal discs (1.3 fold). In order to test the hypothesis that Cyclin G could directly or not, induce its own repression, we designed primers in the 3'UTR to measure expression of the endogenous *CycG* gene. Indeed, expression of endogenous *CycG* was significantly decreased when $CycG^{\Delta P}$ was expressed (Figure 5A and Table S3). Among the 530 genes deregulated in *da-Gal4, UAS-*$CycG^{\Delta P}$*/+* imaginal discs, 216 were up-regulated and 314 down-regulated. Analysis of Gene Ontology (GO) revealed that up-regulated genes were enriched in the categories *cytoplasmic translation* and *translational initiation* whereas down-regulated genes were enriched in the category *mitochondrial respiratory chain complex* (Figure 5B and Table S4). By RT-qPCR, we verified that several ribosomal protein genes (*RpL15, RpL7* and *Rack1*) were over-expressed in *da-Gal4, UAS-*$CycG^{\Delta P}$*/+* imaginal discs (Figure 5C and Table S5).

In conclusion, *CycG*-induced fluctuating asymmetry correlates with activation of genes involved in translation and repression of genes involved in energy production.

Cyclin G binds the Transcriptional Start Sites of many genes also bound by PRC1 and ASX

In order to determine the direct transcriptional targets of Cyclin G, we analysed by ChIP-seq the genome-wide binding sites of Cyclin G in *+/ UAS-Myc-CycG$^{\Delta P}$; da-Gal4/+* imaginal discs. 889 genes with significant peaks at the transcriptional start site (TSS) were recovered (Table S6 and Figures 6A and 6B). ChIP-qPCR analysis of Cyclin G binding on *RPL7, RPL5,* and *Rack1* confirmed that Cyclin peaked on the TSS of these genes and decreased on the gene body (Figure 6C and Table S7). Furthermore, Cyclin G bound its own TSS almost significantly. We then analysed the binding of Cyclin G on its own gene by ChIP-qPCR and verified the presence of Cyclin G on its TSS (Figure 6C and Table S7). As endogenous *CycG* was down-regulated when *CycG$^{\Delta P}$* was expressed, this suggests that Cyclin G represses its own promoter.

The 889 Cyclin G-bound genes were enriched in GO categories *cytoplasmic translation* and *protein phosphorylation* (Figure 6D). Comparison of the 530 genes deregulated in imaginal discs expressing *CycG$^{\Delta P}$* with the 889 genes presenting a peak at the TSS showed that only 62 genes were both deregulated (39 up- and 23 down-regulated) and bound by Cyclin G (Table S8). Strikingly, the 39 up-regulated genes were significantly enriched in the GO category *translation* (GO:0002181~cytoplasmic translation, 14 genes, enrichment score: 11.84, adjusted p-value 2.07E-16).

Using published datasets, we analysed the correlation between regions bound by Cyclin G in *+/UAS-Myc-CycG$^{\Delta P}$; da-Gal/+* imaginal discs and those bound by PRC1, PR-DUB or RNAPolII, or enriched in H3K27me3, in wild type wing imaginal discs (Table S9). Cyclin G-bound regions were significantly exclusive from H3K27me3, corroborating polytene chromosome immunostainings (Dupont et al., 2015). The same comparisons were performed gene-wise and gave the same results. Notably, 80% of Cyclin G-bound genes were bound by RNAPolII (Figure 7). Considering RNAPolII as a proxy for transcriptional activity, we concluded that Cyclin G-bound genes were located in open chromatin and were either paused or transcribed. However, Cyclin G-bound genes were also significantly enriched in PRC1 target genes. Given that PRC1 has the ability to block transcriptional initiation (Dellino et al., 2004), it suggests that Cyclin G-bound genes were most probably paused. Cyclin G also shared many target genes with ASX but, though ASX and Calypso belong to the PR-DUB complex, Cyclin G did not share binding sites with Calypso. This indicates either that the interaction between Cyclin G and ASX

destabilizes the PR-DUB complex or that it takes place outside PR-DUB.

Cyclin G is central in the wing imaginal disc network

These genome-wide analyses indicate that Cyclin G coordinates the expression of genes involved in translation and energy production. However, only a few Cyclin G-bound genes were deregulated in *da-Gal4, UAS-CycG$^{\Delta P}$/+* imaginal discs. To better understand how Cyclin G orchestrates target gene expression, we developed a systems biology approach. We first built an interactome based on genes expressed in control *da-Gal4/+* wing imaginal discs (with a cutoff of 10 reads). Edges corresponding to protein-protein interactions (PPI) and transcription factor-gene interactions (PDI) were integrated into this interactome through DroID (Murali et al., 2011). The resulting wing imaginal disc interactome, further called the WID network, was composed of 9,966 nodes (proteins or genes) connected *via* 56,133 edges (interactions) (WID.xmml file). We then examined the position of Cyclin G in this network. Betweenness centrality - *i.e.* the total number of non-redundant shortest paths going through a certain node – is a measure of centrality in a network (Yu et al., 2007). A node with a high betweenness centrality could control the flow of information across the network (Yamada and Bork, 2009). With 8.32E-03, Cyclin G had one of the highest value of betweenness centrality of the network, ranking at the 30th position among the 9,966 nodes. This suggests that Cyclin G represents a hub in the WID network.

In order to isolate a connected component of the WID network that showed significant expression change when *CycG$^{\Delta P}$* is expressed, we introduced the expression matrix describing expression of the 530 significantly deregulated genes in the WID network. We next used JactiveModules to identify sub-networks of co-deregulated genes (Ideker et al., 2002). A significant sub-network of 222 nodes and 1069 edges centred on Cyclin G was isolated (Z score 48.53). This sub-network was laid out according to functional categories (Figure 8A, CycG_subnetwork.xmml). Four modules composed of genes respectively involved in transcription, mitochondrial activity, translation, and metabolism, were found to be highly connected to Cyclin G. Strikingly, the “translation” module was mainly composed of genes up-regulated in *da-Gal4, UAS-CycG$^{\Delta P}$/+* wing imaginal discs. On the contrary, the “mitochondrion” and “metabolism” modules were mainly composed of genes down-regulated in *da-Gal4, UAS-CycG$^{\Delta P}$/+* wing imaginal discs. Hence, high fluctuating asymmetry of *da-*

Gal4, UAS-CycG$^{\Delta P}$/+ flies correlated positively with the expression of genes involved in translation and negatively with the expression of genes involved in energy production and metabolism. Interestingly, Cyclin G-bound genes in this sub-network were enriched in genes bound by the PRC1 proteins PC, PH and PSC, as well as by RNAPolII, and to a lesser extent by ASX (Figure 8B).

DISCUSSION

The *CycG* gene of *Drosophila melanogaster* encodes a cyclin involved in transcriptional control, cell growth and the cell cycle (Salvaing et al., 2008; Faradji et al., 2011). Mild overexpression of a cDNA encoding Cyclin G deleted of a short C-terminal sequence potentially involved in Cyclin G degradation (a PEST-rich domain; *da-Gal4, UAS-CycG$^{\Delta P}$*/+) induces high fluctuating asymmetry (FA), notably of wings (Debat et al., 2011). Under laboratory conditions (*i.e.* low environmental variation combined with near isogenic lines), this FA should mainly result from developmental noise (Debat and Peronnet, 2013). Thus, *da-Gal4, UAS-CycG$^{\Delta P}$* flies provide a unique tool to investigate the genetic bases of developmental stability. Cyclin G interacts physically with two chromatin regulators of the Enhancers of Trithorax and Polycomb family (ETP), and genetically with many *Polycomb-group* (*PcG*) and *trithorax-group* (*trxG*) genes (Dupont et al., 2015). This prompted us to re-examine *CycG*-induced developmental stability, notably by testing the effect of chromatin regulator mutations, and to investigate deeply the role of Cyclin G in transcriptional regulation.

Cyclin G maintains developmental stability through an organ-autonomous process that involves the PRC1 and PR-DUB complexes

In *Drosophila* very few mutations have been shown to induce an abnormally high FA. Among them are mutations of the gene encoding the *Drosophila* insulin-like peptide 8 (*Dilp8*). Dilp8 participates in systemic coordination of growth. Being produced in growing tissues, it is secreted into the haemolymph and regulates hormone production *via* a well-identified neuronal circuit (Parker and Shingleton, 2011; Garelli et al., 2012; Colombani et al., 2012). Notably, the neurons that produce Lgr3, the Dilp8 receptor, have been identified, and inactivation of *Lgr3* in these neurons also induces high FA. We investigated here the role of *CycG* in this process by deregulating it in the different modules of the circuit. *CycG*-induced wing FA only

occured when the deregulation was local, *i.e.* in wing imaginal discs. More particularly, deregulation of *CycG* in the *Lgr3* neurons did not increase FA. We cannot exclude that Cyclin G induces expression of a systemic factor that is dumped into the haemolymph. However, neither *Dilp8* nor any other insulin-like peptide gene were found deregulated in *da-Gal4, UAS-CycG$^{\Delta P}$* wing imaginal discs. Altogether, these observations suggest that *CycG* maintains developmental stability through an autonomous mechanism which would not involve the systemic *Dilp8/Lgr3* pathway. Such a mechanism recalls Garcia-Bellido's Entelechia model which proposes that local interactions between wing imaginal disc cells, or populations of these cells, orchestrate their own proliferation in order to generate an adult organ of constant size and shape, independently of global cues (García-Bellido and García-Bellido,1998; García-Bellido 2009).

Expression of Cyclin G deleted of the ETP interacting domain doubles FA as compared to expression of Cyclin G with this domain, irrespective of whether the PEST domain is present or not. Hence, the interaction between Cyclin G and chromatin regulators might somehow participate in developmental stability. To test this hypothesis, we combined the *da-Gal4, UAS-CycG$^{\Delta P}$* chromosome and *ETP* or *PcG* mutations. We observed that mutations of the PRC1 and PR-DUB encoding genes strongly increase FA. Moreover, many of the genes that are bound by Cyclin G in wing imaginal discs are also bound by PRC1 and by ASX. Altogether these observations suggest that transcriptional regulation of target genes shared by Cyclin G, PRC1 and ASX is of paramount importance for developmental stability. We did not observe any significant overlap between Cyclin G-bound genes and binding sites for Calypso, the second component of PR-DUB. Yet, *caly* mutations strongly increase *CycG*-induced FA. Thus, the role of PR-DUB in this context remains to be clarified.

PRC1 and PR-DUB contain antagonistic enzymes (SCE/dRing and Calypso) that respectively ubiquitinates and deubiquitinates H2A on lysine 118 in *Drosophila* (lysine 119 in human). Cyclin G co-localizes extensively with H2AK118ub on polytene chromosomes. However, no modification in the global level of H2AK118 ubiquitination was detected in tissues where Cyclin G isoforms were expressed. It was recently shown that canonical PRC1 accounts for only a small fraction of global H2AK118ub, most of this ubiquitination being due to L(3)73Ah, a homolog of mammalian PCGF3 (Lee et al., 2015). Altogether, our data suggest that H2AK118ub

is not involved in developmental stability and rather support the importance of the interaction between Cyclin G and canonical PRC1 in this process. It is tempting to speculate that PRC1 and PR-DUB are partners in the ubiquitination/deubiquitination of an unknown protein important for developmental stability.

Regulation of growth during the cell cycle might be a factor of developmental stability

Additional evidence further connects developmental stability to growth regulation during the cell cycle. Indeed, *CycG*-induced developmental noise is associated with high variance in cell size along with loss of correlation between cell size and cell number (Debat et al., 2011). As Cyclin G is involved in the control of growth in G1 phase of the cell cycle (Faradji et al., 2011), this supports the hypothesis that a mechanism linked to the regulation of cell cycle-dependent growth is essential for developmental stability (Debat et al., 2011). The fact that genes deregulated in wing imaginal discs deregulating *CycG* are involved mainly in translation, energy production and metabolism, strengthens this hypothesis.

It was shown that promoters of actively transcribed genes, notably *GAPDH* and several ribosomal protein genes, are bookmarked by ubiquitination during mitosis (Arora et al., 2012; Arora et al., 2015). This mechanism would allow post-mitotic resumption of their transcription at the very beginning of the G1 phase. Ubiquitination of these genes correlates with active histone marks such as H3K4me3 and H3K36me3 but not with the repressive histone mark H3K27me3. The enzymes responsible for this ubiquitination are the vertebrate PSC homolog BMI1, and Ring1A, one of the SCE/dRing homologs (Arora et al., 2015). In vertebrates, the major PRC1 component that catalyzes H2A ubiquitination is not Ring1A but its homolog Ring1B suggesting that the role of BMI1 and Ring1A in molecular bookmarking are independent of PRC1, and that BMI1 and Ring1A ubiquitinate another chromatin protein (Arora et al., 2015). In *Drosophila,* this role might be played by PRC1 and SCE/dRing. Cyclin G is exclusive of H3K27me3, and binds the promoter of many ribosomal protein genes (Dupont et al., 2015 and the present work). Furthermore, *CycG* deregulation impairs G1 phase progression and cell growth (Faradji et al., 2011). Lastly, the highest FA is observed when Cyclin G lacking the PEST domain, a potential ubiquitination site, is expressed. Hence, an exciting hypothesis would be that Cyclin G is ubiquitinated by PRC1, or PSC and

SCE/dRing outside PRC1, thus releasing the transcriptional standby of active genes at the end of mitosis. In agreement with this, we found that genes involved in metabolism and mitochondrial activity are down-regulated in the *CycG*$^{\Delta P}$ context. However, we observed at the same time that ribosomal protein genes are up-regulated which should rather promote growth. This foreshadows a complex relationship between Cyclin G and the PRC1 and PR-DUB complexes in the cell cycle-dependent regulation of these genes and appeals to the use of a more integrative, systems biology, approach.

Fine-tuned regulation of genes involved in translation, metabolism and mitochondrial activity is necessary for developmental stability

Cyclin G appears central in a small regulatory sub-network that connects genes involved in metabolism, mitochondrial activity and translation. Besides, many of Cyclin G's direct transcriptional targets in this network are also targets of PRC1 and RNAPolII, and to a lesser extent of ASX. Interestingly, it was recently shown by a large scale analysis of the *Drosophila* wing imaginal disc proteome that wing size correlates with some basic metabolic functions, positively with glucose metabolism and negatively with mitochondrial activity, but not with ribosome biogenesis (Okada et al., 2016). In agreement with this, we report here that many genes involved in basic metabolism, such as for example *Gapdh1, Gapdh2* or *Jafrac1,* are down-regulated in the *CycG*$^{\Delta P}$ context, which also agrees with the small mean size of *CycG*$^{\Delta P}$ flies, organs and cells. However, while mitochondrial genes are negatively regulated, ribosomal biogenesis genes are simultaneously positively regulated. Although transcriptome variations are probably not a direct image of proteome variations, our data suggest that robustness of wing size correlates with the fine-tuning of these key functions relative to each other.

Noisiness of gene expression as a source of developmental noise

Cyclin G, PRC1 and PR-DUB are mainly involved in the regulation of transcription. An exciting hypothesis would be that alteration of developmental stability is due to the noisy transcription of their shared targets. *CycG*-induced high FA is associated with high variability of cell size, that might be due to variability in expression of target genes which are mainly involved in growth control. Phenotypic variations in isogenic populations of both prokaryotic and eukaryotic cells may indeed result from

stochastic gene expression mechanisms (McAdams and Arkin, 1997). An increasing corpus of data suggests that the process of gene regulation *per se* can strongly affect variability in gene expression among adjacent cells (for a review see Sanchez et al., 2013). Transcriptional noise may arise at all steps of transcription. For example, the architectural features of promoters have clear effects on mRNA and protein fluctuations in a population of genetically identical cells (Sanchez et al., 2013). RNA polymerase II pausing during elongation is also a source of transcriptional noise (Rajala et al., 2010). In particular, H3K36 methylation, that is related to transcriptional elongation, prevents spurious cryptic transcription from within the gene body (Venkatesh et al., 2012). Recently, activity of the Polycomb complex PRC2 was shown to be important to prevent spurious transcription of inactive genes and to suppress pervasive transcription of intergenic regions (Lee et al., 2015). Mutations of *E(z)* and *esc* that encode two PRC2 members had no effect on *CycG*-induced FA. Dysfunction of PRC2-dependent spurious transcription control is thus unlikely to be the cause of any *CycG*-induced developmental noise. Nevertheless, a similar but weaker effect on intergenic transcription was attributed to PRC1 (Lee et al., 2015). The binding of Cyclin G on many TSS is rather in favor of a role in limiting noisy initiation of transcription. Interestingly, in several cases, noise in gene expression specifically concerns a subset of genes (Weinberger et al., 2012). For example, H3K36 methylation hinders cryptic transcription in a subclass of genes involved in longevity in *S. cerevisiae* and *C. elegans* (Sen et al., 2015). It is thus tempting to speculate that cooperation between Cyclin G and the PRC1 and PR-DUB complexes is important to prevent spurious transcription of genes involved in growth in the broad sense. It will be very interesting to address these points in the future.

MATERIAL AND METHODS

Plasmids

The *pPMW-attB* plasmid was built as follows: Gateway® vector *pPMW* (Invitrogen, a gift from T. Murphy; (Huynh and Zieler, 1999) was linearized by digestion with *NsiI*; the *attB* sequence was amplified from *pUASTattB* (Bischof et al., 2007) using primers *attB-NsiIF* and *attB-NsiIR* (Table S10) and the PCR product was digested with *NsiI*; the digested PCR product and the linearized plasmid were ligated and sequenced. This plasmid was deposited at Addgene (plasmid # 61814).

The full-length *CycG* cDNA (*CycG^{FL}*, encoding the 566 amino-acid protein) was amplified from S2 cell cDNAs using primers *CycGnF* and *CycGnR*. cDNAs encoding truncated forms of Cyclin G (*CycG$^{\Delta P}$*, Cyclin G deleted of the putative PEST domain corresponding to amino-acids 542 to 566; *CycG$^{\Delta E}$*, Cyclin G deleted of the ETP-interacting domain corresponding to amino-acids 1 to 130; *CycG$^{\Delta E\Delta P}$*, Cyclin G deleted of both domains) were amplified from the full-length *CycG* cDNA using primers *CycGnF* and *CycG541R*, *CycG130F* and *CycGnR*, and *CycG130F* and *CycG541R*, respectively (Table S10 and Dupont et al., 2015). The PCR products were cloned into *pENTR/D-TOPO*® (Invitrogen), transferred into *pPMW-attB* and the resulting plasmids *pPMW-attB-CycG^{FL}*, *pPMW-attB-CycG$^{\Delta P}$*, *pPMW-attB-CycG$^{\Delta E}$*, *pPMW-attB-CycG$^{\Delta E\Delta P}$* were sequenced.

Drosophila melanogaster strains and genetics

Flies were raised on standard yeast-cornmeal medium at 25°C.

Myc-CycG transgenic lines were obtained by *PhiC31*-integrase mediated insertion into strain *y^{1}M{vas-int.Dm}ZH-2Aw*;M{3xP3-RFP.attP'}ZH-51C* (stock BL-24482). Plasmids *pPMW-attB-CycG^{FL}*, *pPMW-attB-CycG$^{\Delta P}$*, *pPMW-attB-CycG$^{\Delta E}$* and *pPMW-attB-CycG$^{\Delta E\Delta P}$* were injected into embryos, G0 adults were back-crossed to *yw*, and G1 transformants were crossed to *yw* again to obtain G2 transformants (BestGene Inc.). Transformants were individually crossed with *yw; Sp/CyO*, and the curly wing siblings were crossed with each other. Homozygous transgenic lines were then obtained by crossing 5 females and 5 males. The resulting lines were named *UAS-Myc-CycG^{FL}, UAS-Myc-CycG$^{\Delta P}$, UAS-Myc-CycG$^{\Delta E}$* and *UAS-Myc-CycG$^{\Delta E\Delta P}$*.

To estimate fluctuating asymmetry (FA), five replicate crosses were performed for each genotype, wherein 6 females carrying a Gal4 driver were mated with 5 males carrying a *CycG* transgene. Parents were transferred into a new vial every 48 h (three times) then discarded. 30 females were then sampled from the total offspring. Gal4 drivers used were *daughterless-Gal4* (*da-Gal4*) (Wodarz et al., 1995), *nubbin-Gal4* (*nub-Gal4*), *optomotor-blind-Gal4* (*omb-Gal4*), *rotund-Gal4* (*rn-Gal4*), *scalloped-Gal4* (*sd-Gal4*), *teashirt-Gal4* (*tsh-Gal4*), *vestigial-Gal4* (*vg-Gal4*) (from the Bloomington *Drosophila* stock center), and *Insulin-like peptide 3-Gal4* (*dILP3-Gal4*), *neuropeptide F-Gal4* (*NPF-Gal4*), *Pigment-dispersing factor-Gal4* (*Pdf-Gal4*), *period-Gal4* (*per-Gal4*), *phantom-Gal4* (*phm-Gal4*), *Prothoracicotropic hormone-Gal4* (*Ptth-Gal4*), *R10B09-Gal4*, kind gifts from Dr Maria Dominguez's lab (Ferres-Marco et al.,

2006).

The *da-Gal4, UAS-CycG$^{\Delta P}$* third chromosome, obtained by recombination of *da-Gal4* with the original *UAS-CycG$^{\Delta P}$* transgene (*RCG76*), was used to test genetic interactions between *CycG* and several *PcG* or *ETP* mutations (Dupont et al., 2015). Alleles used are described in (Soto et al., 1995; Beuchle et al., 2001;Salvaing et al., 2006; Gaytán de Ayala Alonso et al., 2007; Fritsch et al., 2003; Gutiérrez et al., 2012) (Table 3). To estimate FA, 5 crosses were performed for each genotype, wherein 6 *PcG* or *ETP* mutant females were mated with 5 *da-Gal4, UAS-CycG$^{\Delta P}$* males, the parents were transferred into a new vial every 48 h (three times) then discarded. 30 females combining the *PcG* or *ETP* mutation and *da-Gal4 UAS-CycG$^{\Delta P}$* were sampled from the offspring. *PcG* and *ETP* mutant females were crossed with *da-Gal4* in parallel to measure FA of heterozygous mutants.

Morphometrics

Right and left wings of sampled females were mounted on slides, dorsal side up, in Hoyer's medium. Slides were scanned with a Hamamatsu Nanozoomer Digital Slide scanner, running the Nanozoomer software with a 20x objective and an 8-bit camera. Wing pictures were separately exported into tif format using NDP.view and the 5x lens. All wings were oriented with the hinge to the left. Image J was used to digitize 15 landmarks or only landmarks 3 and 13 when indicated (Figure 1B). Analysis of size FA was performed as described previously (Debat et al., 2011) using the FA10 index as FA estimator, *i.e.* FA corrected for measurement error, directional asymmetry and inter-individual variation (Palmer and Strobeck, 1992). For all genotypes, the interaction individual*side was significant, indicating that FA was larger than measurement error.

RNA-seq experiments and RT-qPCR validations

Wing imaginal discs from *da-Gal4/UAS-CycG$^{\Delta P}$* and *da-Gal4/+* third instar female larvae were dissected, and total RNAs were extracted as previously described except that 150 discs homogenized by pipetting were used for each extraction (Coléno-Costes et al., 2012). Three biological replicates were generated for each genotype. Library preparation and Illumina sequencing were performed at the Ecole Normale Supérieure Genomic Platform (Paris, France). Messenger (polyA+) RNAs were purified from 1 µg of total RNA using oligo(dT). Libraries were prepared using the

strand specific RNA-Seq library preparation TruSeq Stranded mRNA kit (Illumina). Libraries were multiplexed by 6 on 2 flowcell lanes. A 50 bp single read sequencing was performed on a HiSeq 1500 device (Illumina). A mean of 38.1 ± 4.8 million reads was obtained for each of the 6 samples (Table S11). They were aligned with the *Drosophila melanogaster* genome (dm6, r6.07) using TopHat 2 (v2.0.10) (Kim et al., 2013). Unambiguously mapping reads (a mean of 24.9 ± 4.9 million reads) were then assigned to genes and exons described by the Ensembl BDGP5 v77 assembly, by using the "summarizeOverlaps" function from the "GenomicAlignments" package (v 1.2.2) in "Union" mode (Lawrence et al., 2013). Library size normalization and differential expression analysis were both performed with DESeq 2 (v 1.6.3) and genes with adjusted p-value below 0.05 were retained as differentially expressed (Love et al., 2014). Gene Ontology analysis was performed using DAVID (Huang et al., 2009; Huang et al., 2009).

For RT-qPCR validations, RNAs were treated with Turbo DNAse (Ambion), and cDNA were synthesized with SuperScript II Reverse transcriptase (Invitrogen) using random primers. RT-qPCR experiments were carried out in a CFX96 system (Bio-Rad) using SsoFast EvaGreen Supermix (Bio-Rad). Three biological replicates were performed for each genotype. Expression levels were quantified with the Pfaffl method (Bustin et al., 2009). The geometric mean of two reference genes, *Lamin* (*Lam*) and *rasputin* (*rin*), the expression of which did not vary when *CycG*$^{\Delta P}$ was expressed, was used for normalization (Vandesompele et al., 2002). Sequences of primer couples are listed in Table S10.

An interactome was built using Cytoscape (v 2.8.3) and the DroID plugin (v 1.5) to introduce protein-protein and transcription factor-gene interactions (Murali et al., 2011). The jActiveModules plugin (v 2.23) was used to find sub-networks of co-deregulated genes in the interactome by using "overlap threshold" 0.8, "score adjusted for size", and "regional scoring" (Ideker et al., 2002).

ChIP-seq experiments and ChIP-qPCR validations

Wing imaginal discs from *+/UAS-Myc-CycG*$^{\Delta P}$*;; +/da-Gal4* and *+/da-Gal4* third instar female larvae were used for chromatin immunoprecipitation (ChIP).

For ChIP-seq experiments, 600 wing imaginal discs were dissected (taking one disc per larva) in Schneider medium and aliquoted per 50 in 1.5 mL microtubes on ice. The 12 microtubes were treated as described in (Coléno-Costes et al., 2012)

with minor modifications. Discs were fixed at 22°C. 12 sonication cycles were performed (Diagenode Bioruptor sonifier; cycles of 30" ON, 30" OFF, high power). After centrifugation, the 12 supernatants were pooled, homogenized, and 2% were removed (Input). The remaining fragmented chromatin was redistributed into 12 tubes and each tube was adjusted to 1 mL with 140 mM NaCl, 10 mM Tris-HCl pH 8.0, 1 mM EDTA, 1% Triton X-100, 0.1% sodium deoxycholate, 0.1% BSA, Roche complete EDTA-free protease inhibitor cocktail). For immunoprecipitation, 3 µg of anti-Myc antibody (Abcam 9132) were added per tube. The of water. Two biological replicates were performed.

Library preparation and Illumina sequencing were performed at the Ecole normale superieure Genomic Platform (Paris, France). Libraries were prepared using NEXTflex ChIP-Seq Kit (Bioo Scientific), using 38 ng of IP or Input DNA. Libraries were multiplexed by 10 on one flowcell run. A 75 bp single read sequencing was performed on a NextSeq 500 device (Illumina). Reads were filtered by the "fastq_quality_filter" command from the "fastx-Toolkit" package (http://hannonlab.cshl.edu/fastx_toolkit/), using a threshold of 90% bases with mapping quality ≥ 20. A mean of 55.6 ± 15.2 million reads was obtained for each of the 4 samples (Table S12). Reads that successfully passed the filtering step were aligned to the *Drosophila* genome (dm6, r6.07) using Bowtie 2 (http://bowtie-bio.sourceforge.net/bowtie2/) (v2.1.0) with default parameters (Langmead and Salzberg, 2012). Peaks were called by MACS2 (v2.1.0) by comparing each ChIP to its input library, with fragment size fixed at 110 bp and otherwise default parameters (Zhang et al., 2008) . Peak reproducibility between the two biological replicates was then analysed with the IDR method (https://www.encodeproject.org/software/idr/) (Li et al., 2011). Briefly, an IDR score was assigned to each peak by the "batch-consistency-analysis" function, using the recommended parameters for MACS peaks (peak ranking based on p-value). Peaks below the 0.05 threshold were considered reproducible. The overlapping reproducible peaks from both replicates were fused using the BEDtools suite "merge" function (Quinlan and Hall, 2010), resulting in the final list of peaks kept for subsequent analysis. Cyclin G-bound genes were defined as genes from the genome annotation file (dm6, r6.07) which overlapped at least one of these Cyclin G peaks, as obtained by the BEDtools suite "intersect" function (Quinlan and Hall, 2010).

For ChIP-qPCR validations, ChIP were performed similarly with the anti-Myc antibody. Rabbit IgG (Diagenode) were used as a negative control (mock). qPCR experiments were carried out in a CFX96 system (Bio-Rad) using SsoFast EvaGreen Supermix (Bio-Rad). Sequences of primer couples are listed in Table S10. Data were normalized against Input chromatin.

Heatmaps and aggregation plots of Cyclin G signal over gene bodies and Transcription Start Sites (TSS) were generated using the ngsplot package. (https://github.com/shenlab-sinai/ngsplot) (Shen et al., 2014). Some genes with spurious signal (such as genes from the histone complex) were excluded from the analysis based on signal uniformity over the full length of the gene (cumulative derivative of Cyclin G signal over gene length = 0).

Data access

High-throughput sequencing data have been submitted to GEO. Accession numbers for RNA-seq data: GSE99462, GSM2644389, GSM2644390, GSM2644391, GSM2644392, GSM2644393, GSM2644394. Accession number for ChIP-seq data: GSE99461, GSM2644385, GSM2644386, GSM2644387, GSM2644388.

Genomic association

Genomic loci enriched for Polycomb (PC), Posterior Sex Comb (PSC), Polyhomeotic (PH), RNA Polymerase II (RNAPolII) and H3K27me3 in wild type imaginal discs of third instar larvae were retrieved from GEO (GSE42106) (Schaaf et al., 2013) (H3K27me3_WholeWingDisc GSM1032567, PcRJ_AnteriorWingDisc GSM1032571, PcRJ_PosteriorWingDisc GSM1032574, Ph_WholeWingDisc GSM1032576, PolII_WholeWingDisc GSM1032577, Psc_WholeWingDisc GSM1032578. Binding sites for PC in the whole wing disc were defined as the overlap between PC binding sites in the anterior and posterior wing disc compartment, as obtained by the BEDtools "intersect" function. For ASX and Calypso, the bed files were a kind gift from Dr. Jürg Müller (Scheuermann et al., 2010). The mappability file for dm6 genome with 25 nt reads (the smallest size in the compared data) was generated using the Peakseq code (http://archive.gersteinlab.org/proj/PeakSeq/Mappability_Map/Code/). The overall size of the mappable genome was used as the effective genome size for the GAT software (https://github.com/AndreasHeger/gat) to assess the significance of the overlap between peaks of Cyclin G and other factors

(Heger et al., 2013). As GAT performs a two-tailed test, it displays low p-values both for significant overlap and exclusion (as between Cyclin G and H3K27me3).

Gene overlap significance assessment was made as follows: under the null hypothesis, genes that are enriched for ASX, Calypso, PC, PSC, PH, RNAPolII or H3K27me3 in wild type imaginal discs of third instar larvae should not exhibit any bias towards Cyclin G targets. Thus, the overlap between $\mathbf{n}$ enriched genes and $\mathbf{K}$ Cyclin G targets genes should be explained by random sampling without replacement of $\mathbf{n}$ genes within the total amount $\mathbf{N}$ of *Drosophila melanogaster* genes. The amount of overlap under the null hypothesis $\mathbf{X}$ follows a hypergeometric law: $X \sim HY(K, N, n)$. The significance of the observed overlap $\mathbf{k}$ was computed as the probability of observing $\mathbf{X}$ higher or equal to $\mathbf{k}$ under the null hypothesis: $\mathrm{P}(\mathrm{X} \geq \mathrm{k})$.

Acknowledgments

We thank Dr. Emmanuèle Mouchel-Vielh and Dr. Jean-Michel Gibert for stimulating discussions and critical reading of the manuscript, the Bloomington Stock Center for fly strains, Dr. Jürg Müller for the alleles of *Asx* and *caly* and for the ASX and Calypso ChIP bed files, Dr. Maria Dominguez and Dr Sergio Juarez-Carreño for the *dilp3-Gal4, R19B09-Gal4, npf-Gal4, pdf-Gal4, per-Gal4, ptth-Gal4* and *tsh-Gal4* drivers. This work was funded by the Centre National de la Recherche Scientifique (CNRS), Université Pierre et Marie Curie (UPMC), Sorbonne Universités (grant SU-14-R-CDV-05-1 to FP), and Fondation ARC pour la Recherche sur le Cancer (grant PJA20131200314 to FP). The École Normale Supérieure genomic platform was supported by the France Génomique national infrastructure, funded as part of the "Investissements d'Avenir" program managed by the Agence Nationale de la Recherche (contract ANR-10-INBS-09). CAD was funded by a doctoral fellowship from the MESR (Ministère de l'Enseignement Supérieur et de la Recherche). JD was funded by a doctoral fellowship from the MESR and by the Fondation pour la Recherche médicale (FDT20160435164).

References

Adler, P.N., Charlton, J., and Brunk, B. (1989). Genetic interactions of the *suppressor 2 of zeste* region genes. *Dev Genet 10*, 249-260. doi:10.1002/dvg.1020100314

Arora, M., Packard, C.Z., Banerjee, T., and Parvin, J.D. (2015). RING1A and BMI1 bookmark active genes via ubiquitination of chromatin-associated proteins. *Nucleic Acids Res 44*, 2136-2144. 10.1093/nar/gkv1223

Arora, M., Zhang, J., Heine, G.F., Ozer, G., Liu, H.W., Huang, K., and Parvin, J.D. (2012). Promoters active in interphase are bookmarked during mitosis by ubiquitination. *Nucleic Acids Res 40*, 10187-0202. doi:10.1093/nar/gks820

Barabasi, A.L., and Albert, R. (1999). Emergence of scaling in random networks. *Science 286*, 509-512.

Beck, S., Faradji, F., Brock, H., and Peronnet, F. (2010). Maintenance of Hox gene expression patterns. *Adv Exp Med Biol 689*, 41-62.

Beuchle, D., Struhl, G., and Müller, J. (2001). Polycomb group proteins and heritable silencing of *Drosophila* Hox genes. *Development 128*, 993-1004.

Bischof, J., Maeda, R.K., Hediger, M., Karch, F., and Basler, K. (2007). An optimized transgenesis system for *Drosophila* using germ-line-specific *varphiC31* integrases. *Proceedings of the National Academy of Sciences 104*, 3312-17.

Breuker, C.J., Patterson, J.S., and Klingenberg, C.P. (2006). A single basis for developmental buffering of *Drosophila* wing shape. *PLoS One 1*, e7. doi:10.1371/journal.pone.0000007

Bustin, S.A., Benes, V., Garson, J.A., Hellemans, J., Huggett, J., Kubista, M., Mueller, R., Nolan, T., Pfaffl, M.W., et al. (2009). The MIQE guidelines: minimum information for publication of quantitative real-time PCR experiments. *Clin Chem 55*, 611-622. doi:10.1373/clinchem.2008.112797

Coléno-Costes, A., Jang, S.M., de Vanssay, A., Rougeot, J., Bouceba, T., Randsholt, N.B., Gibert, J.M., Le Crom, S., Mouchel-Vielh, E., et al. (2012). New partners in regulation of gene expression: the Enhancer of Trithorax and Polycomb Corto interacts with methylated Ribosomal Protein L12 via its chromodomain. *PLoS Genet 8*, e1003006. doi:10.1371/journal.pgen.1003006

Colombani, J., Andersen, D.S., and Léopold, P. (2012). Secreted peptide Dilp8 coordinates Drosophila tissue growth with developmental timing. Science *336*, 582-85. doi:10.1126/science.1216689

Debat, V., and Peronnet, F. (2013). Asymmetric flies: The control of developmental noise in *Drosophila. Fly* (Austin) *7*, 1-8. doi: 10.4161/fly.23558

Debat, V., Bloyer, S., Faradji, F., Gidaszewski, N., Navarro, N., Orozco-Terwengel, P., Ribeiro, V., Schlötterer, C., Deutsch, J.S., and Peronnet, F. (2011). Developmental Stability: A Major Role for Cyclin G in *Drosophila melanogaster*. *PLoS Genet 7*, e1002314. doi:10.1371/journal.pgen.1002314

Debat, V., Milton, C.C., Rutherford, S., Klingenberg, C.P., and Hoffmann, A.A. (2006). Hsp90 and the quantitative variation of wing shape in *Drosophila melanogaster. Evolution 60*, 2529-538.

Dellino, G.I., Schwartz, Y.B., Farkas, G., McCabe, D., Elgin, S.C., and Pirrotta, V. (2004). Polycomb silencing blocks transcription initiation. *Mol Cell 13*, 887-893.

Dongen, S.V. (2006). Fluctuating asymmetry and developmental instability in evolutionary biology: past, present and future. *J Evol Biol 19*, 1727-743. doi:10.1111/j.1420-9101.2006.01175.x

Dupont, C.A., Dardalhon-Cuménal, D., Kyba, M., Brock, H.W., Randsholt, N.B., and Peronnet, F. (2015). *Drosophila* Cyclin G and epigenetic maintenance of gene expression during development. *Epigenetics Chromatin 8*, 18. doi:10.1186/s13072-015-0008-6

Faradji, F., Bloyer, S., Dardalhon-Cuménal, D., Randsholt, N.B., and Peronnet, F. (2011). *Drosophila melanogaster* Cyclin G coordinates cell growth and cell proliferation. *Cell Cycle 10*, 1-14. Erratum (2014) *Cell Cycle 13*, 2480-2480.

Feder, M.E., and Hofmann, G.E. (1999). Heat-shock proteins, molecular chaperones, and the stress response: evolutionary and ecological physiology. *Annual review of physiology 61*, 243-282.

Ferres-Marco, D., Gutierrez-Garcia, I., Vallejo, D.M., Bolivar, J., Gutierrez-Aviño, F.J., and Dominguez, M. (2006). Epigenetic silencers and Notch collaborate to promote malignant tumours by Rb silencing. *Nature 439*, 430-36. doi:10.1038/nature04376

Fritsch, C., Beuchle, D., and Müller, J. (2003). Molecular and genetic analysis of the Polycomb group gene *Sex combs extra/Ring* in *Drosophila. Mech Dev 120*, 949-954. doi:10.1016/s0925-4773(03)00083-2

García-Bellido, A. (2009). The cellular and genetic bases of organ size and shape in *Drosophila. Int J Dev Biol 53*, 1291-1303. doi:10.1387/ijdb.072459ag

García-Bellido, A.C., and García-Bellido, A. (1998). Cell proliferation in the

attainment of constant sizes and shapes: the Entelechia model. *Int J Dev Biol 42*, 353-362.

Garelli, A., Gontijo, A.M., Miguela, V., Caparros, E., and Dominguez, M. (2012). Imaginal discs secrete insulin-like peptide 8 to mediate plasticity of growth and maturation. *Science 336*, 579-582. doi:10.1126/science.1216735

Gaytán de Ayala Alonso, A., Gutiérrez, L., Fritsch, C., Papp, B., Beuchle, D., and Müller, J. (2007). A genetic screen identifies novel polycomb group genes in *Drosophila. Genetics 176*, 2099-2108. doi:10.1534/genetics.107.075739

Geisler, S.J., and Paro, R. (2015). Trithorax and Polycomb group-dependent regulation: a tale of opposing activities. *Development 142*, 2876-887. doi:10.1242/dev.120030

Gildea, J.J., Lopez, R., and Shearn, A. (2000). A screen for new trithorax group genes identified little imaginal discs, the *Drosophila melanogaster* homologue of human retinoblastoma binding protein 2. *Genetics 156*, 645-663.

Graveley, B.R., Brooks, A.N., Carlson, J.W., Duff, M.O., Landolin, J.M., Yang, L., Artieri, C.G., van Baren, M.J., Boley, N., et al. (2011). The developmental transcriptome of *Drosophila melanogaster. Nature 471*, 473-79. doi:10.1038/nature09715

Grimaud, C., Negre, N., and Cavalli, G. (2006). From genetics to epigenetics: the tale of Polycomb group and trithorax group genes. *Chromosome Res 14*, 363-375. doi:10.1007/s10577-006-1069-y

Grossniklaus, U., and Paro, R. (2014). Transcriptional Silencing by Polycomb-Group Proteins. *Cold Spring Harb Perspect Biol 6*. doi:10.1101/cshperspect.a019331

Gutiérrez, L., Oktaba, K., Scheuermann, J.C., Gambetta, M.C., Ly-Hartig, N., and Müller, J. (2012). The role of the histone H2A ubiquitinase Sce in Polycomb repression. *Development 139*, 117-127. doi:10.1242/dev.074450

Heger, A., Webber, C., Goodson, M., Ponting, C.P., and Lunter, G. (2013). GAT: a simulation framework for testing the association of genomic intervals. *Bioinformatics 29*, 2046-48. doi:10.1093/bioinformatics/btt343

Huang, D.W., Sherman, B.T., and Lempicki, R.A. (2009). Systematic and integrative analysis of large gene lists using DAVID bioinformatics resources. *Nat Protoc 4*, 44-57. doi:10.1038/nprot.2008.211

Huang, D.W., Sherman, B.T., and Lempicki, R.A. (2009). Bioinformatics enrichment tools: paths toward the comprehensive functional analysis of large gene lists.

Nucleic Acids Res 37, 1-13. doi:10.1093/nar/gkn923

Huynh, C.Q., and Zieler, H. (1999). Construction of modular and versatile plasmid vectors for the high-level expression of single or multiple genes in insects and insect cell lines. *J Mol Biol 288*, 13-20.

Ideker, T., Ozier, O., Schwikowski, B., and Siegel, A.F. (2002). Discovering regulatory and signalling circuits in molecular interaction networks. *Bioinformatics 18 Suppl 1*, S233-240.

Kim, D., Pertea, G., Trapnell, C., Pimentel, H., Kelley, R., and Salzberg, S.L. (2013). TopHat2: accurate alignment of transcriptomes in the presence of insertions, deletions and gene fusions. *Genome Biol 14*, R36. doi:10.1186/gb-2013-14-4-r36

Kingston, R.E., and Tamkun, J.W. (2014). Transcriptional Regulation by Trithorax-Group Proteins. *Cold Spring Harb Perspect Biol 6* doi:10.1101/cshperspect.a019349

Kitano, H. (2004). Biological robustness. *Nat Rev Genet 5*, 826-837. doi:10.1038/nrg1471

Langmead, B., and Salzberg, S.L. (2012). Fast gapped-read alignment with Bowtie 2. *Nat Methods 9*, 357-59. doi:10.1038/nmeth.1923

Lawrence, M., Huber, W., Pagès, H., Aboyoun, P., Carlson, M., Gentleman, R., Morgan, M.T., and Carey, V.J. (2013). Software for computing and annotating genomic ranges. *PLoS Comput Biol 9*, e1003118. doi:10.1371/journal.pcbi.1003118

Leamy, L., Klingenberg, C., Sherratt, E., Wolf, J., and Cheverud, J. (2015). The Genetic Architecture of Fluctuating Asymmetry of Mandible Size and Shape in a Population of Mice: Another Look. *Symmetry 7*, 146-163. doi:10.3390/sym7010146

Leamy, L.J., Routman, E.J., and Cheverud, J.M. (2002). An epistatic genetic basis for fluctuating asymmetry of mandible size in mice. *Evolution 56*, 642-653. doi:10.1038/sj.hdy.6800637

Leamy, L.J., Workman, M.S., Routman, E.J., and Cheverud, J.M. (2005). An epistatic genetic basis for fluctuating asymmetry of tooth size and shape in mice. *Heredity* (Edinb) *94*, 316-325. doi:10.1038/sj.hdy.6800637

Leamy, L.J.L., and Klingenberg, C.P.K. (2005). The genetics and evolution of fluctuating asymmetry. *Annu. Rev. Ecol. Evol. Syst. 36*, 1-21. doi:10.1146/annurev.ecolsys.36.102003.152640

Lee, H.G., Kahn, T.G., Simcox, A., Schwartz, Y.B., and Pirrotta, V. (2015). Genome-wide activities of Polycomb complexes control pervasive transcription. *Genome Res 25*,1170-81. doi: 10.1101/gr.188920.11

Levy, S.F., and Siegal, M.L. (2008). Network hubs buffer environmental variation in *Saccharomyces cerevisiae. PLoS Biol 6*, e264. doi:10.1371/journal.pbio.0060264

Li, Q., Brown, J.B., Huang, H., and Bickel, P.J. (2011). Measuring reproducibility of high-throughput experiments. *The annals of applied statistics 5*, 1752-779.

Love, M.I., Huber, W., and Anders, S. (2014). Moderated estimation of fold change and dispersion for RNA-seq data with DESeq2. *Genome Biol 15*, 550. doi:10.1186/s13059-014-0550-8

McAdams, H.H., and Arkin, A. (1997). Stochastic mechanisms in gene expression. Proc Natl Acad Sci USA *94*, 814-19.

Milton, C.C., Huynh, B., Batterham, P., Rutherford, S.L., and Hoffmann, A.A. (2003). Quantitative trait symmetry independent of Hsp90 buffering: distinct modes of genetic canalization and developmental stability. *Proc Natl Acad Sci USA 100*, 13396-3401. doi:10.1073/pnas.1835613100

Murali, T., Pacifico, S., Yu, J., Guest, S., Roberts, G.G., and Finley, R.L. (2011). DroID 2011: a comprehensive, integrated resource for protein, transcription factor, RNA and gene interactions for *Drosophila*. *Nucleic Acids Res 39*, D736-743. doi:10.1093/nar/gkq1092

Neto-Silva, R.M., Wells, B.S., and Johnston, L.A. (2009). Mechanisms of growth and homeostasis in the *Drosophila* wing. *Annu Rev Cell Dev Biol 25*, 197-220. doi:10.1146/annurev.cellbio.24.110707.175242

Newman, M.E.J. (2003). The structure and function of complex networks. *SIAM Review 45*, 167-256.

Nijhout, F., and Davidowitz, G. (2003). Developmental Perspectives on Phenotypic Variation, Canalization, and Fluctuating Asymmetry. In Developmental instability, causes and consequences, M. Polak, eds. (New York: Oxford University Press).

Okada, H., Ebhardt, H.A., Vonesch, S.C., Aebersold, R., and Hafen, E. (2016). Proteome-wide association studies identify biochemical modules associated with a wing-size phenotype in *Drosophila melanogaster. Nat Commun 7*, 12649. doi:10.1038/ncomms12649

Palmer, A.R., and Strobeck, C. (1992). Fluctuating asymmetry as a measure of developmental stability: Implications of non-normal distributions and power of

statistical tests. *Acta Zool. Fennica 191*, 57-72.

Palmer, R.A. (1994). Fluctuating asymmetry analysis: a primer. In Developmental Instability: Its Origins and Evolutionary Implications (T. A. Markow. Netherlands, Kluwer Academic Publishers).

Parker, N.F., and Shingleton, A.W. (2011). The coordination of growth among Drosophila organs in response to localized growth-perturbation. *Dev Biol 357*, 318-325. doi:10.1016/j.ydbio.2011.07.002

Pengelly, A.R., Kalb, R., Finkl, K., and Müller, J. (2015). Transcriptional repression by PRC1 in the absence of H2A monoubiquitylation. *Genes Dev 29*, 1487-492. doi:10.1101/gad.265439.115

Queitsch, C., Sangster, T.A., and Lindquist, S. (2002). Hsp90 as a capacitor of phenotypic variation. *Nature 417*, 618-624. doi:10.1038/nature749

Quinlan, A.R., and Hall, I.M. (2010). BEDTools: a flexible suite of utilities for comparing genomic features. *Bioinformatics 26*, 841-42.

Rajala, T., Häkkinen, A., Healy, S., Yli-Harja, O., and Ribeiro, A.S. (2010). Effects of transcriptional pausing on gene expression dynamics. *PLoS Comput Biol 6*, e1000704. doi:10.1371/journal.pcbi.1000704

Rutherford, S, Hirate, Y, and Swalla, BJ (2007). The Hsp90 capacitor, developmental remodeling and evolution: The robustness of gene networks and the curious evolvability of metamorphosis. Cr*it Rev Biochem Mol 42*, 355-372.

Rutherford, S., Knapp, J.R., and Csermely, P. (2007). Hsp90 and developmental networks. *Adv Exp Med Biol 594*, 190-97. doi:10.1007/978-0-387-39975-1_16

Rutherford, S.L., and Lindquist, S. (1998). Hsp90 as a capacitor for morphological evolution. *Nature 396*, 336-342. doi:10.1038/24550

Salvaing, J., Decoville, M., Mouchel-Vielh, E., Bussière, M., Daulny, A., Boldyreva, L., Zhimulev, I., Locker, D., and Peronnet, F. (2006). Corto and DSP1 interact and bind to a maintenance element of the *Scr* Hox gene: understanding the role of Enhancers of trithorax and Polycomb. *BMC Biol 4*, 9. doi:10.1186/1741-7007-4-9

Salvaing, J., Nagel, A.C., Mouchel-Vielh, E., Bloyer, S., Maier, D., Preiss, A., and Peronnet, F. (2008a). The enhancer of trithorax and polycomb corto interacts with cyclin G in *Drosophila. PLoS One 3*, e1658. doi:10.1371/journal.pone.0001658

Salvaing, J., Mouchel-Vielh, E., Bloyer, S., Preiss, A., and Peronnet, F. (2008b). Regulation of Abd-B expression by Cyclin G and Corto in the abdominal epithelium of Drosophila. *Hereditas 145*, 138-146. doi:HRD2067

[pii]10.1111/j.0018-0661.2008.02067.x

Sanchez, A., Choubey, S., and Kondev, J. (2013). Regulation of noise in gene expression. *Annu Rev Biophys 42*, 469-491. doi:10.1146/annurev-biophys-083012-130401

Sangster, T.A., Salathia, N., Undurraga, S., Milo, R., Schellenberg, K., Lindquist, S., and Queitsch, C. (2008). HSP90 affects the expression of genetic variation and developmental stability in quantitative traits. *Proc Natl Acad Sci USA 105*, 2963-68. doi:10.1073/pnas.0712200105

Schaaf, C.A., Misulovin, Z., Gause, M., Koenig, A., Gohara, D.W., Watson, A., and Dorsett, D. (2013). Cohesin and polycomb proteins functionally interact to control transcription at silenced and active genes. *PLoS Genet 9*, e1003560. doi:10.1371/journal.pgen.1003560

Scheuermann, J.C., de Ayala Alonso, A.G., Oktaba, K., Ly-Hartig, N., McGinty, R.K., Fraterman, S., Wilm, M., Muir, T.W., and Müller, J. (2010). Histone H2A deubiquitinase activity of the Polycomb repressive complex PR-DUB. *Nature 465*, 243-47. doi:10.1038/nature08966

Scheuermann, J.C., Gutiérrez, L., and Müller, J. (2012). Histone H2A monoubiquitination and Polycomb repression: the missing pieces of the puzzle. *Fly* (Austin) *6*, 162-68. doi:10.4161/fly.20986

Sen, P., Dang, W., Donahue, G., Dai, J., Dorsey, J., Cao, X., Liu, W., Cao, K., Perry, R., et al. (2015). H3K36 methylation promotes longevity by enhancing transcriptional fidelity. *Genes Dev 29*, 1362-376. doi:10.1101/gad.263707.115

Shen, L., Shao, N., Liu, X., and Nestler, E. (2014). ngs.plot: Quick mining and visualization of next-generation sequencing data by integrating genomic databases. *BMC Genomics 15*, 284. doi:10.1186/1471-2164-15-284

Siegal, M.L., and Bergman, A. (2002). Waddington's canalization revisited: developmental stability and evolution. *Proc Natl Acad Sci USA 99*, 10528-532. doi:10.1073/pnas.102303999

Simon, J., Chiang, A., and Bender, W. (1992). Ten different Polycomb group genes are required for spatial control of the abdA and AbdB homeotic products. *Development 114*, 493-505.

Soto, M.C., Chou, T.B., and Bender, W. (1995). Comparison of germline mosaics of genes in the Polycomb group of *Drosophila melanogaster. Genetics 140*, 231-243.

Takahashi, H., Okada, Teramura, and Tsujino (2011). Deficiency mapping of the genomic regions associated with effects on developmental stability in *Drosophila melanogaster. Evolution 65*, 3565-577.

Vallejo, D.M., Juarez-Carreño, S., Bolivar, J., Morante, J., and Dominguez, M. (2015). A brain circuit that synchronizes growth and maturation revealed through Dilp8 binding to Lgr3. *Science 350*, aac6767. doi: 10.1126/science.aac6767.

Vandesompele, J., De Preter, K., Pattyn, F., Poppe, B., Van Roy, N., De Paepe, A., and Speleman, F. (2002). Accurate normalization of real-time quantitative RT-PCR data by geometric averaging of multiple internal control genes. *Genome Biol 3*, research0034.1-c0034.11.

Van Valen, L. (1962). A study of fluctuating asymmetry. *Evolution 16*, 125-142.

Venkatesh, S., Smolle, M., Li, H., Gogol, M.M., Saint, M., Kumar, S., Natarajan, K., and Workman, J.L. (2012). Set2 methylation of histone H3 lysine 36 suppresses histone exchange on transcribed genes. *Nature 489*, 452-55. doi:10.1038/nature11326

Weinberger, L., Voichek, Y., Tirosh, I., Hornung, G., Amit, I., and Barkai, N. (2012). Expression Noise and Acetylation Profiles Distinguish HDAC Functions. *Mol Cell 47*, 193-202. doi:10.1016/j.molcel.2012.05.008

Wodarz, A., Hinz, U., Engelbert, M., and Knust, E. (1995). Expression of crumbs confers apical character on plasma membrane domains of ectodermal epithelia of *Drosophila. Cell 82*, 67-76.

Yamada, T., and Bork, P. (2009). Evolution of biomolecular networks: lessons from metabolic and protein interactions. *Nat Rev Mol Cell Biol 10*, 791-803. doi:10.1038/nrm2787

Yeyati, P.L., Bancewicz, R.M., Maule, J., and van Heyningen, V. (2007). Hsp90 selectively modulates phenotype in vertebrate development. *PLoS Genet 3*, e43. doi:10.1371/journal.pgen.0030043

Yu, H., Kim, P.M., Sprecher, E., Trifonov, V., and Gerstein, M. (2007). The importance of bottlenecks in protein networks: correlation with gene essentiality and expression dynamics. *PLoS Comput Biol 3*, e59. doi:10.1371/journal.pcbi.0030059

Zhang, Y., Liu, T., Meyer, C.A., Eeckhoute, J., Johnson, D.S., Bernstein, B.E., Nusbaum, C., Myers, R.M., Brown, M., et al. (2008). Model-based analysis of ChIP-Seq (MACS). *Genome Biol 9*, R137. doi:10.1186/gb-2008-9-9-r137

Figures

Figure 1: Acquisition of morphometric data.

A – Superimposition of the left and right wings of a sample of *da-Gal4, UAS-CycG*$^{\Delta P}$ flies (left wings in red, right wings in green) showing high asymmetry.

B - Red dots show the 15 landmarks digitized on the wings. FA10 was computed using these landmarks obtained from the left and right wings of at least 30 females randomly sampled from the population as described (Debat et al., 2011).

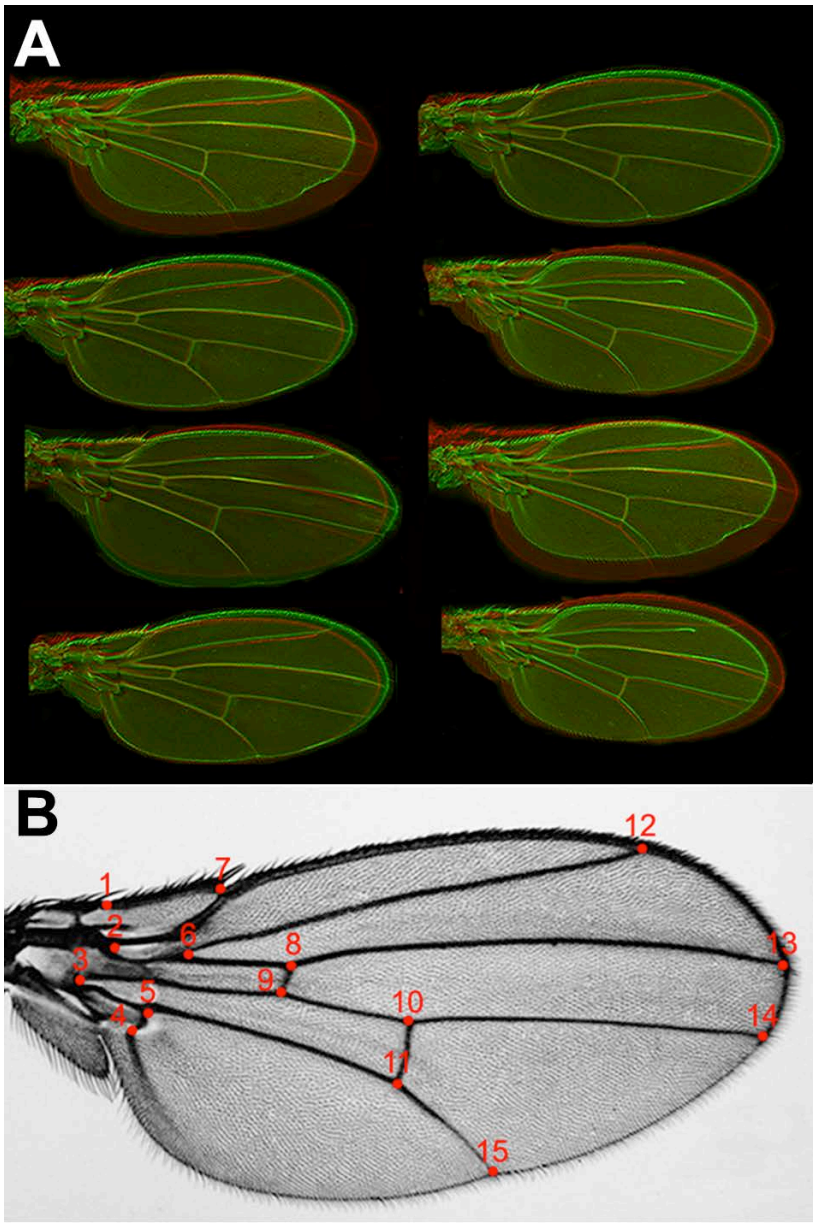

Figure 2: Local deregulation of *CycG* induces high fluctuating asymmetry.

A – Wing length fluctuating asymmetry (FA10) of females bearing a Gal4 driver either associated with *UAS-CycG$^{\Delta P}$* (dark orange) or alone (light orange). Wing length was measured as the distance between landmarks 3 and 13. *** p-value<0.001.

B – Expression of the driver genes in 3rd instar larva wing imaginal discs (dark grey) and central nervous system (light grey) as indicated in modENCODE (Graveley et al., 2011).

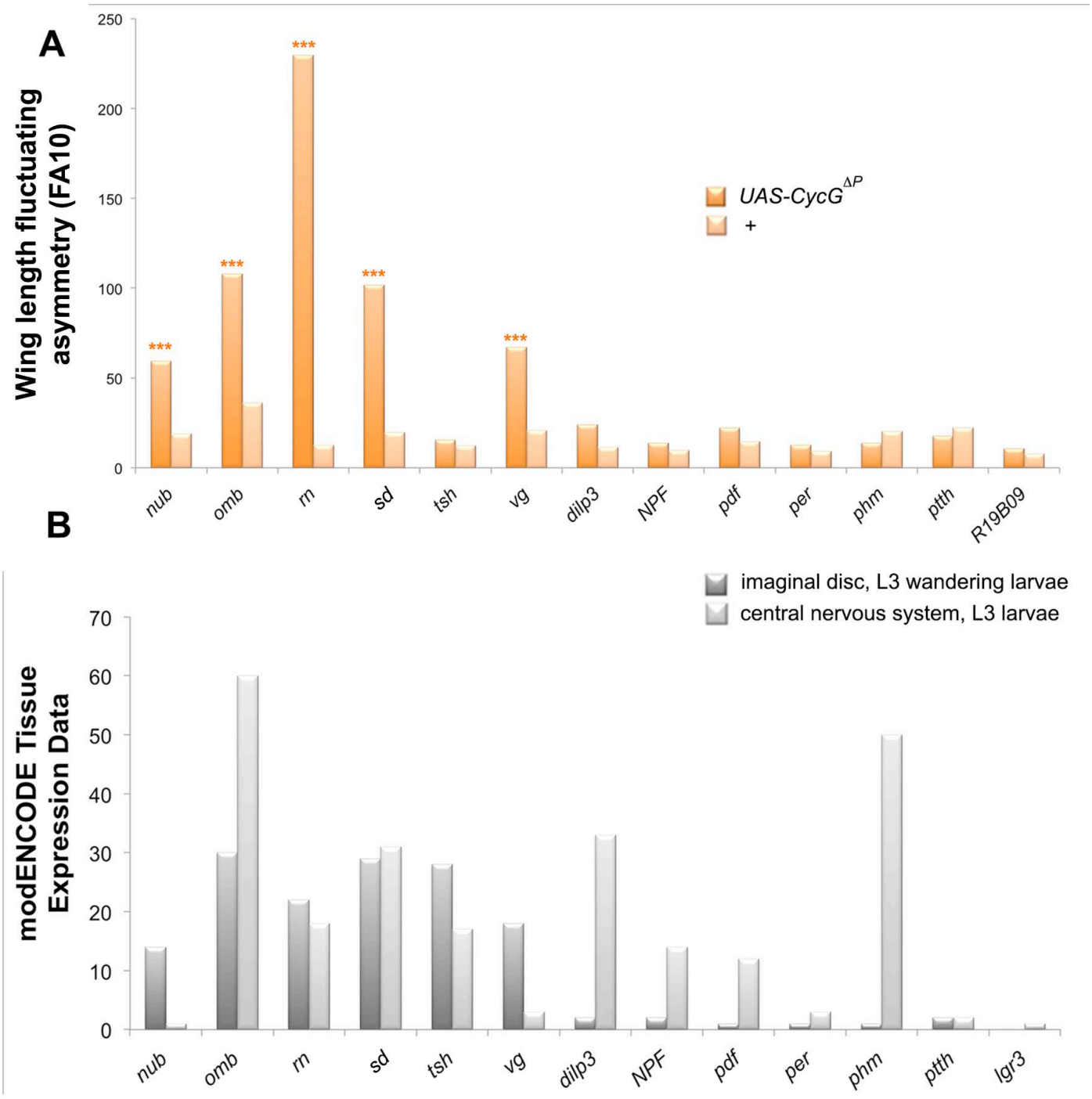

Figure 3: The ETP interacting domain limits *CycG*-induced fluctuating asymmetry

A – Centroid size fluctuating asymmetry (FA10) of females *da-Gal4*/+ (+), *+/UAS-Myc-CycG^{FL}; da-Gal4/+*, (*CycG^{FL}*) and *+/UAS-Myc-CycG$^{\Delta E}$*; *da-Gal4,* (*CycG$^{\Delta E}$*).

B – Centroid size fluctuating asymmetry (FA10) of females *da-Gal4*/+ (+), *+/ UAS-Myc-CycG$^{\Delta P}$; da-Gal4/+* (*CycG$^{\Delta P}$*) and *+/UAS-Myc- CycG$^{\Delta E\Delta P}$; da-Gal4/+* (*CycG$^{\Delta E\Delta P}$*).

*** p-value<0.001.

Wing centroid size was calculated using the 15 landmarks described in Figure 1B.

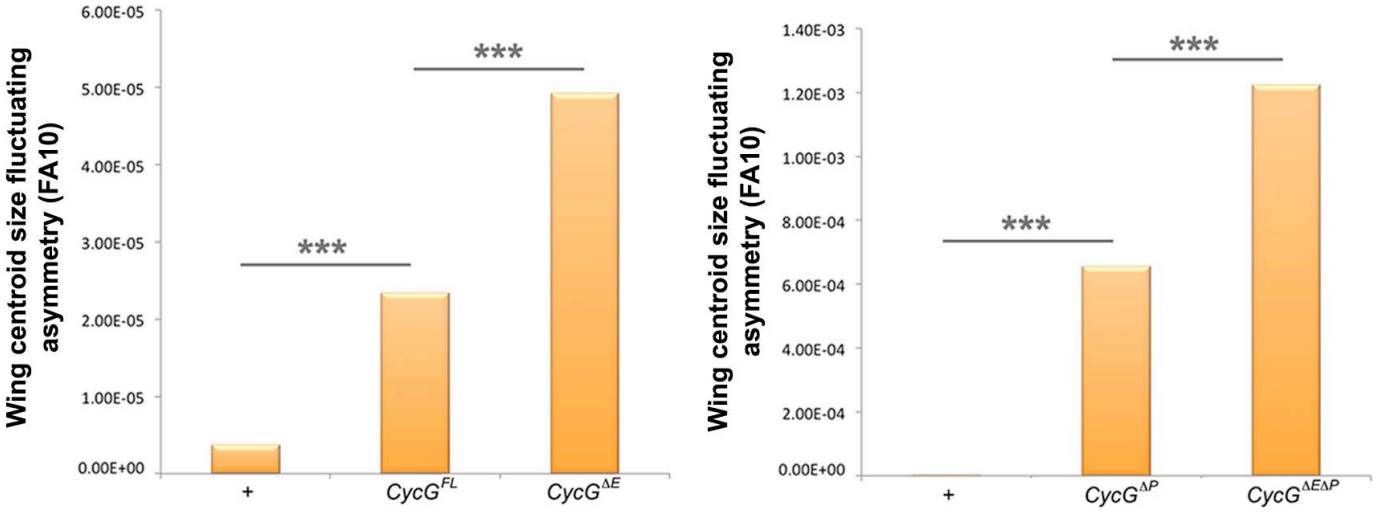

Figure 4: *CycG* interacts with several *PcG* and *ETP* genes for developmental stability.

Centroid size fluctuating asymmetry (FA10) of *ETP* or *PcG* heterozygous mutant females combined with *da-Gal4, UAS-CycG$^{\Delta P}$* (dark orange; *da-Gal4, UAS-CycG$^{\Delta P}$*; *PcG/+* or *da-Gal4, UAS-CycG$^{\Delta P}$*; *ETP/+*) and *ETP* or *PcG* heterozygous mutant females combined with *da-Gal4* (light orange; *da-Gal4/+; PcG/+* or *da-Gal4*; *ETP/+*). In brown (+), centroid size fluctuating asymmetry of *da-Gal4, UAS-CycG$^{\Delta P}$/+* and *da-Gal4/+* females.

*p-value<0.05; ** p-value<0.01; *** p-value<0.001.

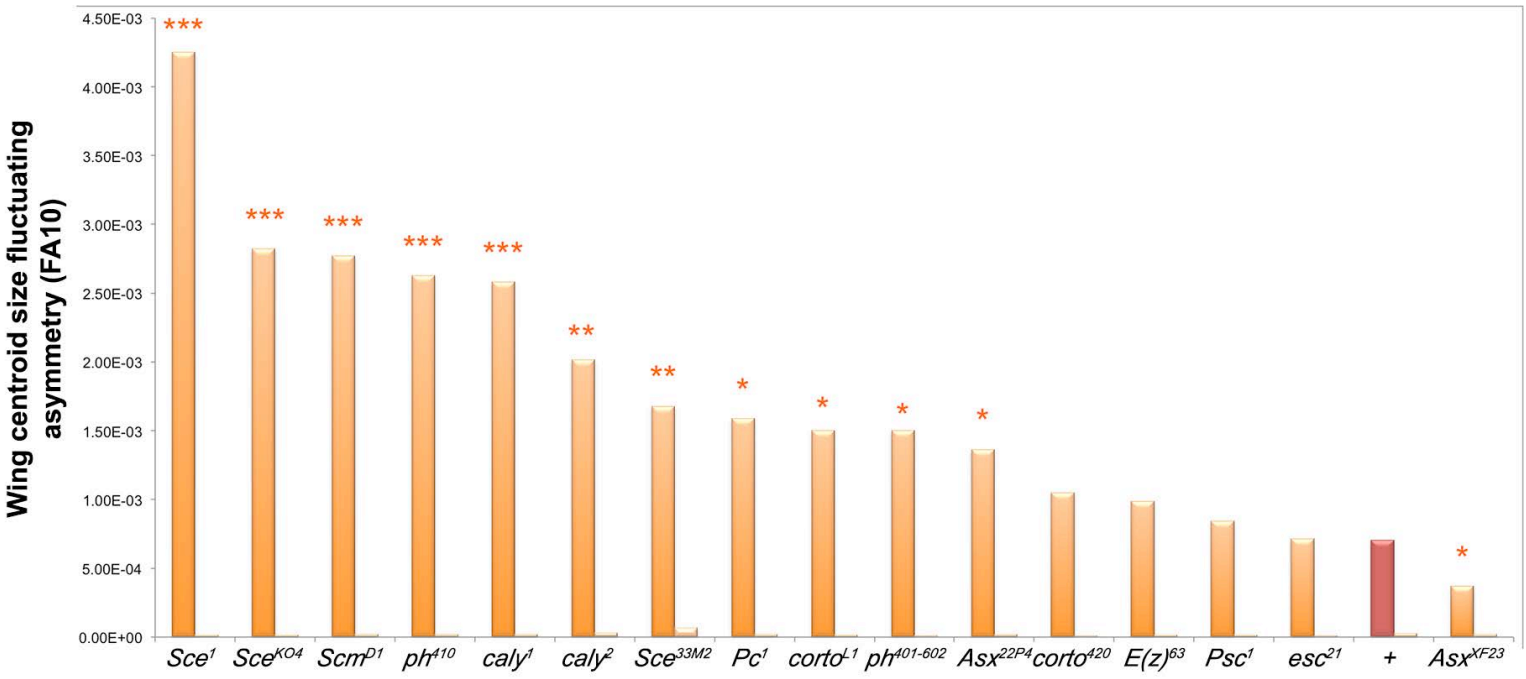

Figure 5: Genes deregulated in wing imaginal discs expressing *CycG$^{\Delta P}$*.

A – RT-qPCR analysis of endogenous *CycG* expression in *da-Gal4,UAS-CycG$^{\Delta P}$/+* and *da-Gal4/+* wing imaginal discs. ** p-value<0.01.

B – Ontology of up-regulated and down-regulated genes in *da-Gal4, UAS-CycG$^{\Delta P}$/+ versus da-Gal4/+* wing imaginal discs. Gene ontology analysis was performed with DAVID (Huang et al., 2009; Huang et al., 2009).

C – RT-qPCR analysis of *RPL15*, *RPL7* and *Rack1* expression in *da-Gal4, UAS-CycG$^{\Delta P}$/+* and *da-Gal4/+* wing imaginal discs. ** p-value<0.01; *** p-value<0.001.

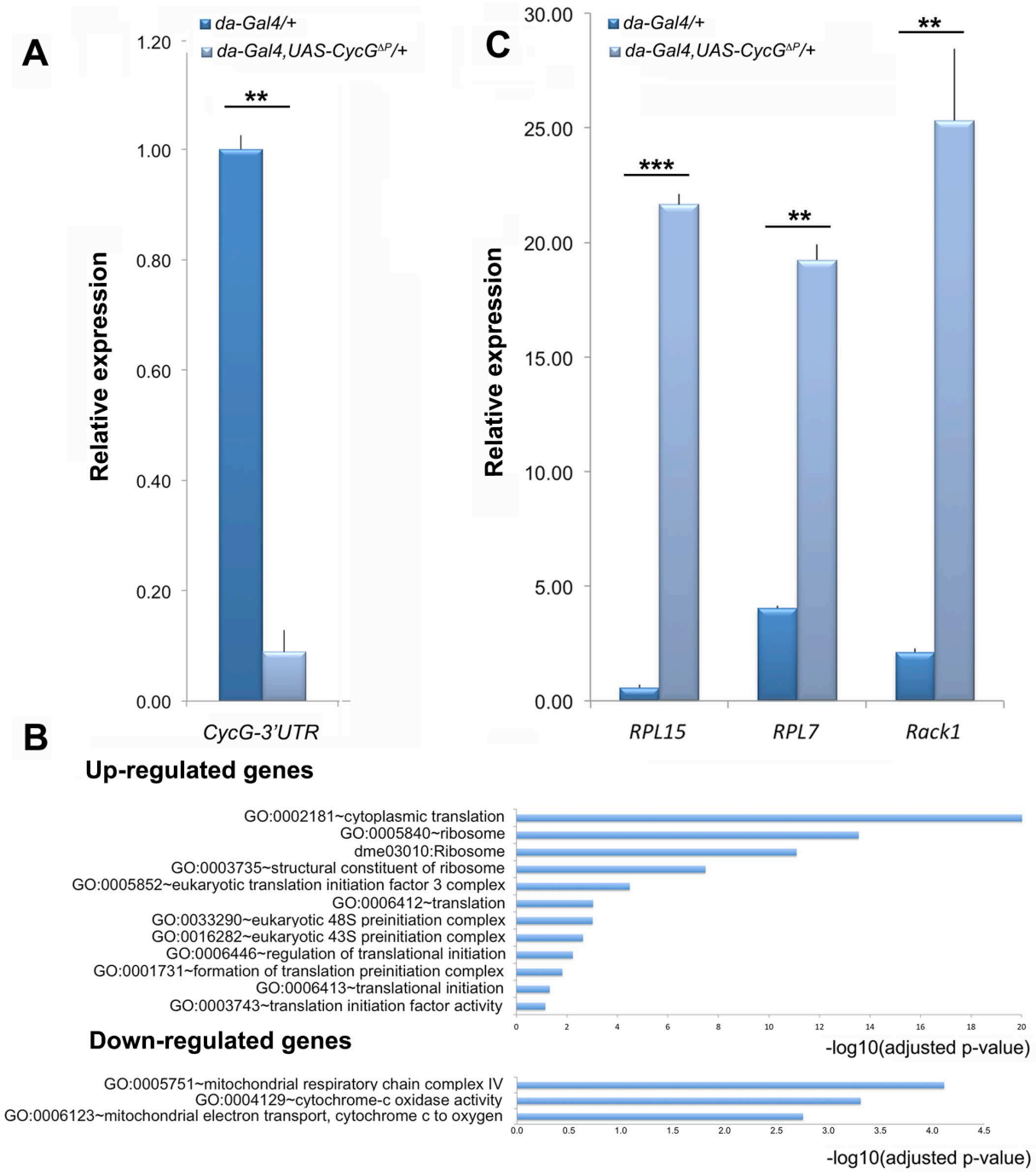

Figure 6: Identification of Cyclin G genome-wide binding sites in wing imaginal discs.

A – Heat-map showing the enrichment of Cyclin G over the Input signal on the TSS of 889 genes. TSS: Transcriptional Start Site; TES: Transcriptional End Site.

B – Average profile of Cyclin G signal over these genes shown as an aggregation plot.

C – ChIP-qPCR analysis of *RPL7, RPL5, Rack1* and *CycG*. IPs were performed either with Myc antibody (α-Myc) to reveal the presence of Cyclin G, or with rabbit IgG as negative control (mock). qPCR were performed using oligonucleotide primers located either at the TSS or in the gene body as indicated in Table S1.

D – Ontology of the 889 genes. Gene ontology analysis was performed with DAVID (Huang et al., 2009; Huang et al., 2009).

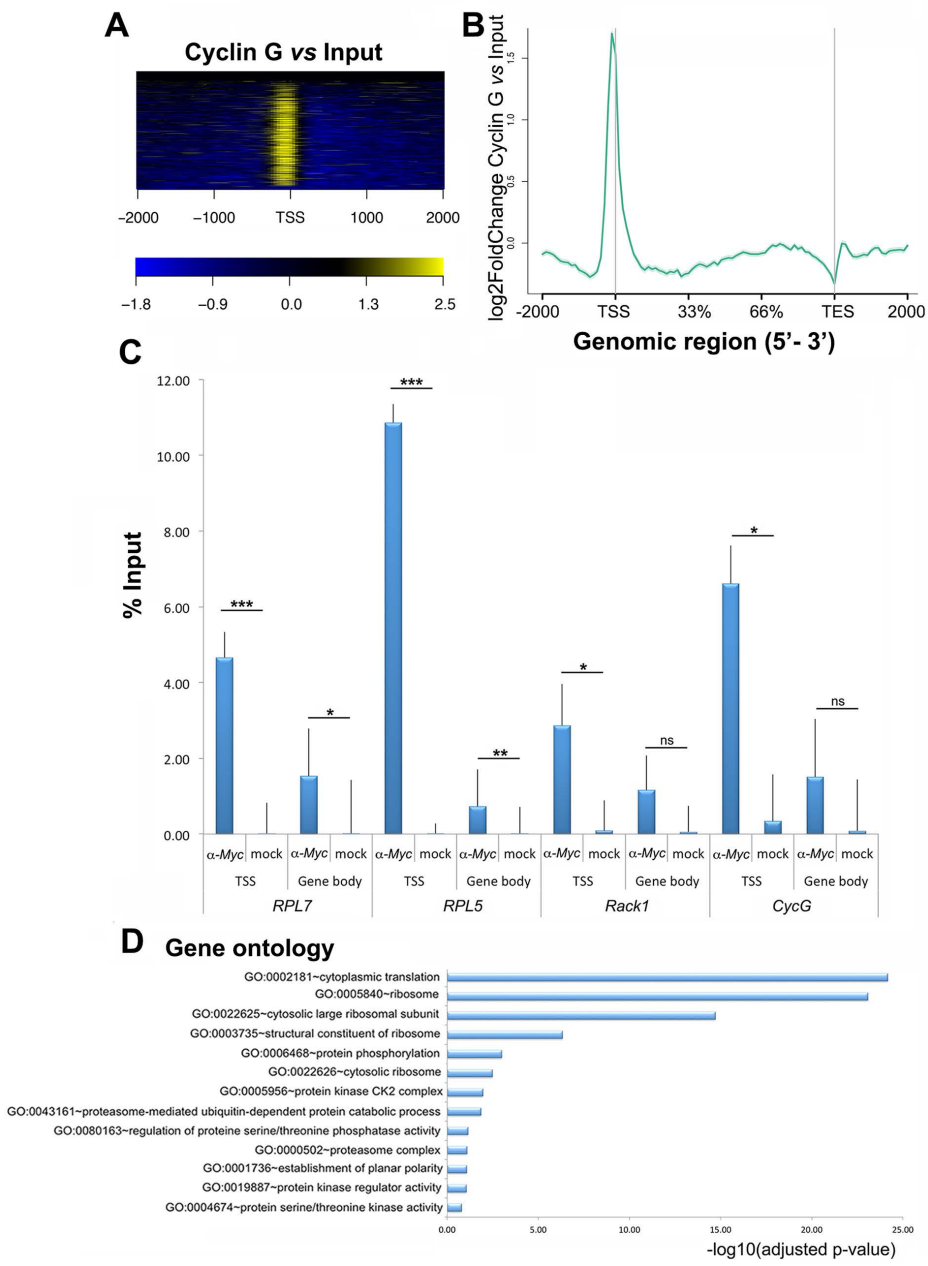

Figure 7: Cyclin G shares target genes with PRC1, ASX and RNAPolII but not with Calypso.

Venn diagrams showing the intersection between Cyclin G-bound genes in *+/ UAS-Myc-CycG$^{\Delta P}$; da-Gal4/+,* wing imaginal discs and PH, PC, PSC, ASX, Calypso and RNApolII in wild-type wing imaginal discs.

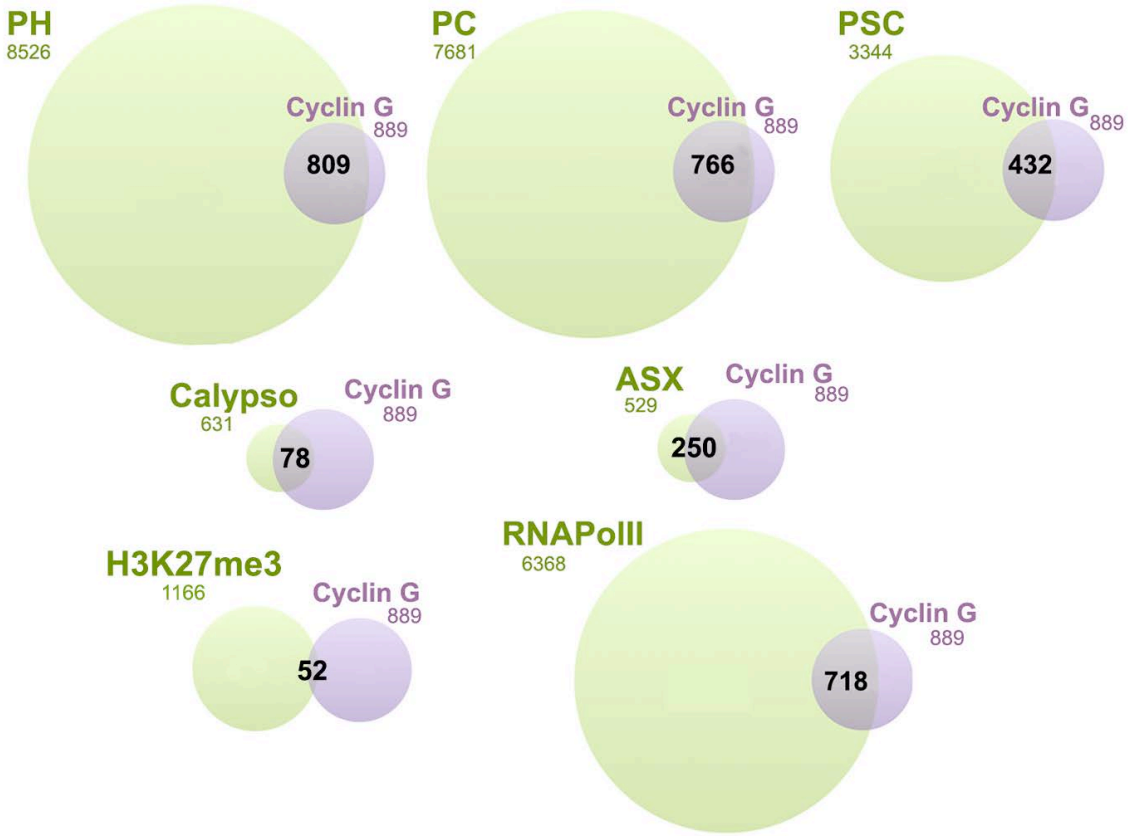

Figure 8: Functional subnetwork identified in wing imaginal discs expressing *CycG$^{\Delta P}$*.

A – Schematic representation of a sub-network of 222 genes centred on Cyclin G and identified using JactiveModules (Z score 48.53) (Ideker et al., 2002). In this sub-network, 65 genes were up-regulated in *da-Gal4, UAS-CycG$^{\Delta P}$ versus da-Gal4/+* wing imaginal discs (green gradient), 124 genes were down-regulated (red gradient), and 33 genes were not significantly deregulated (grey). Genes bound by Cyclin G are circled in red. Transcription factor genes are represented by squares. Genes were clustered depending on their function. Black edges correspond to interactions discovered in the present study. Grey edges correspond to interactions described in the literature and imported into the WID network using DroID (Murali et al., 2011).

B – Genes bound by ASX, Calypso, PC, PH, PSC, or RNAPolII, or enriched in H3K27me3 in the sub-network are represented in red.

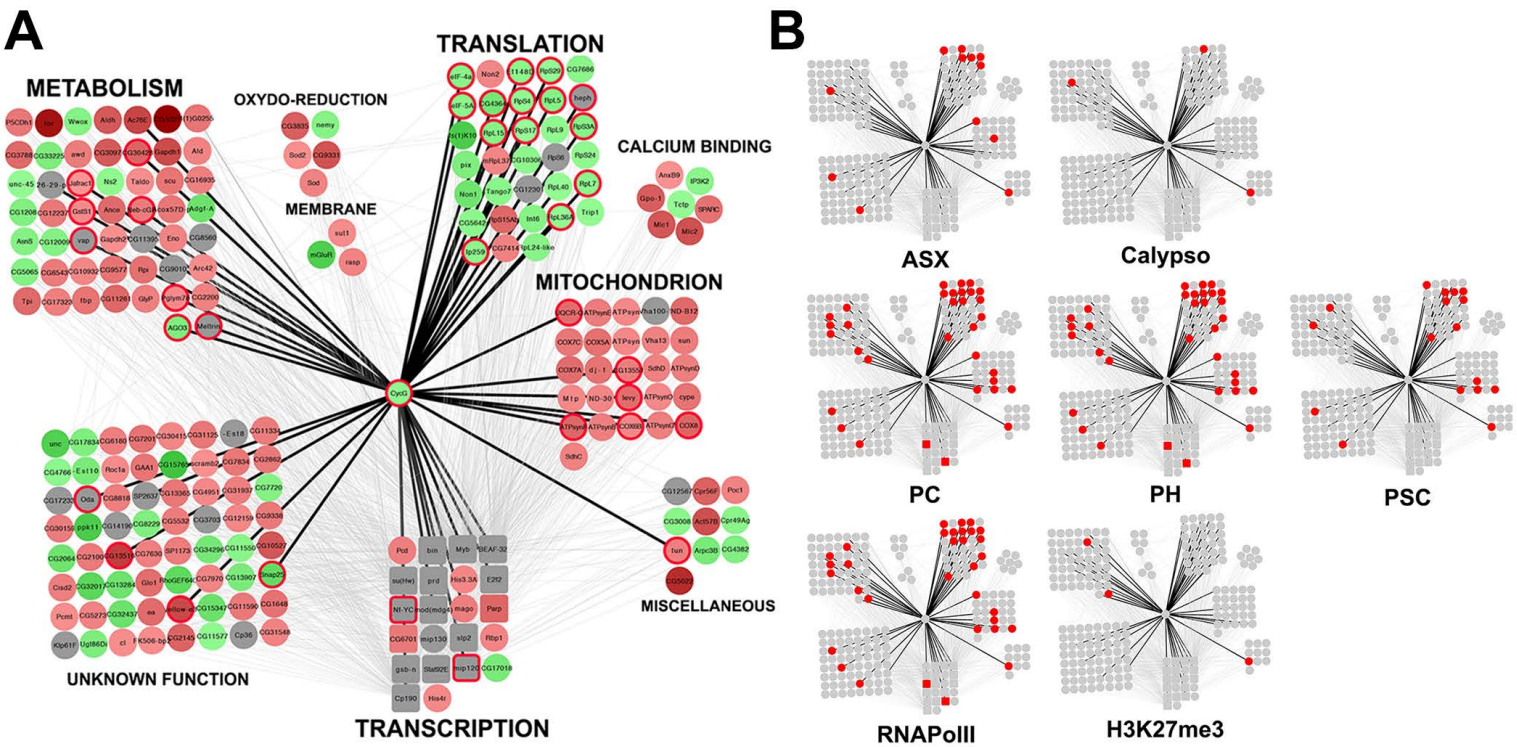

Table 1: Size fluctuating asymmetry of flies expressing *CycG*$^{\Delta P}$ with different Gal4 drivers.

Size fluctuating asymmetry was estimated with the FA10 index using landmarks 3 and 13 (Palmer and Strobeck, 1992) as described previously (Debat et al., 2011). 30 females of each genotype were measured.

Standard F-tests were used to compare FA values between genotypes. Df: degrees of freedom. *CycG*$^{\Delta P}$: cDNA encoding the protein deleted of the PEST domain.

	FA10		Df			
	UAS-CycG$^{\Delta P}$	+	*UAS-CycG*$^{\Delta P}$	+	F	p-value
nub-Gal4	59.34	18.80	26.25	26.45	3.1561	2.34E-03
omb-Gal4	107.90	36.17	28.41	27.88	2.9829	2.87E-03
rn-Gal4	229.69	12.59	28.80	25.30	18.2390	9.60E-11
sd-Gal4	101.85	19.83	28.56	26.45	5.1367	3.64E-05
tsh-Gal4	15.49	12.32	23.89	22.27	1.2576	2.97E-01
vg-Gal4	67.11	20.90	28.45	26.67	3.2107	1.88E-03
dilp3-Gal4	23.90	11.51	26.97	23.71	2.0776	4.02E-02
NPF-Gal4	13.90	9.90	25.09	22.98	1.4048	2.12E-01
pdf-Gal4	22.14	14.75	24.60	25.09	1.5012	1.60E-01
per-Gal4	12.69	9.09	23.12	21.53	1.3963	2.23E-01
phm-Gal4	13.81	20.18	23.86	27.06	1.4609	1.80E-01
ptth-Gal4	17.62	22.14	25.17	26.30	1.2565	3.39E-01
R19B09-Gal4	10.76	7.81	23.15	21.87	1.3782	2.32E-01

Table 2: Centroid size fluctuating asymmetry of flies expressing different versions of Cyclin G.

Centroid size fluctuating asymmetry was estimated with the FA10 index using the 15 landmarks (Palmer and Strobeck, 1992) as described previously (Debat et al., 2011). Standard F-tests were used to compare FA values between genotypes. Df: degrees of freedom. n: number of females analysed. *CycG*^{FL}: cDNA encoding the full-length protein; *CycG*$^{\Delta E}$: cDNA encoding a protein deleted of the ETP-interacting domain; *CycG*$^{\Delta P}$: cDNA encoding a protein deleted of the PEST domain; *CycG*$^{\Delta E \Delta P}$: cDNA encoding a protein deleted of both domains.

				yw; +/da-Gal4		*yw; +/UAS-CycG^{FL}; da-Gal4/+*		*yw; +/UAS-CycG$^{\Delta E}$; da-Gal4/+*		*yw; +/UAS-CycG$^{\Delta P}$; da-Gal4/+*	
Genotype	n	FA10	Df	F	p-value	F	p-value	F	p-value	F	p-value
yw; da-Gal4/+	146	3.73E-06	16.37	-	-						
yw; +/UAS-CycG^{FL}; da-Gal4/+	89	2.34E-05	72.82	6.27	9.30E-05	-	-				
yw; +/UAS-CycG$^{\Delta E}$; da-Gal4/+	88	4.92E-05	85.78	13.19	4.49E-07	2.10	6.96E-04	-			
yw; +/UAS-CycG$^{\Delta P}$; da-Gal4/+	111	6.57E-04	108.76	176.01	7.08E-16	28.06	4.52E-35	13.34	6.63E-28	-	-
yw; +/UAS-CycG$^{\Delta E \Delta P}$; +/da-Gal4	95	1.22E-03	93.28	328.22	5.34E-18	52.32	7.18E-44	24.88	1.12E-37	1.86	9.32E-04

Table 3: Polycomb and Enhancer of Polycomb and Trithorax alleles used in this study.

Class	Gene	Allele	Allele class	Reference
ETP	*Additional sex combs*	*Asx^{22P4}*	no protein detected	Scheuermann et al., 2010
		Asx^{XF23}	loss of function	Simon et al., 1992
	corto	*$corto^{420}$*	loss of function	Salvaing et al., 2006
		$corto^{L1}$	amorphic	Salvaing et al., 2006
PcG	*calypso*	*$caly^{1}$*	no protein detected	Gaytán de Ayala Alonso et al., 2007; Scheuermann et al., 2010
	calypso	*$caly^{2}$*	no protein detected	Gaytán de Ayala Alonso et al., 2007; Scheuermann et al., 2010
	Enhancer of zeste	*$E(z)^{63}$*	loss of function	Beuchle et al., 2001
	extra sexcombs	*esc^{21}*	amorphic	Gindhart and Kaufman, 1995
	Polycomb	*Pc^{1}*	amorphic	Capdevilla et al., 1986
	polyhomeotic	*$ph\text{-}d^{401}ph\text{-}p^{602}$*	null	Dura et al., 1987
	polyhomeotic proximal	*$ph\text{-}p^{410}$*	loss of function	Dura et al., 1987
	Posterior sex combs	*Psc^{1}*	hypomorphic	Adler et al., 1989
	Sex combs extra	*Sce^{1}*	null	Gorfinkiel et al., 2004
	Sex combs extra	*Sce^{33M2}*	loss of function	Fritsch et al., 2003
	Sex combs extra	*Sce^{KO4}*	null	Gutiérrez et al., 2012
	Sex comb on midleg	*Scm^{D1}*	amorphic	McKeon and Brock, 1991,